Process Improvement for Plywood Product Manufacturing Using Design of Experiments

Ladan Zamirian

A thesis
in
The Department
of
Mechanical, Industrial and Aerospace Engineering (MIAE)

Presented in Partial Fulfillment of the Requirements
For the Degree of Master of Applied Science
Concordia University
Montréal, Québec, Canada

September 2020

Concordia University
School of Graduate Studies

This is to certify that the thesis prepared

By: **Ladan Zamirian**

Entitled: **Process Improvement for Plywood Product Manufacturing Using Design of Experiments**

and submitted in partial fulfillment of the requirements for the degree of

Master of Applied Science

complies with the regulations of this University and meets the accepted standards with respect to originality and quality.

Signed by the final Examining Committee:

_____ Chair
Dr. Akif A. Bulgak

_____ Examiner
Dr. Akif A. Bulgak

_____ Examiner
Dr. Farnoosh Naderkhani

_____ Supervisor
Dr. Mingyuan Chen

Approved by _____
Dr. Mamoun Medraj Chair of Department or Graduate Program Director

_____
Dr. Mourad Debbabi Dean, Gina Cody School of Engineering and Computer Science

Date _____

Abstract

Process Improvement for Plywood Product Manufacturing Using Design of Experiments

Ladan Zamirian

Delamination is the most common defect in plywood manufacturing. In this thesis, a simulation study of plywood pressing process is conducted to study the impact of critical parameters causing delamination of a certain type of plywood product in mass production. This research work is conducted on specifically the adhesive and pressing step as most of the delamination defects are observed. The modeling of the hot pressing of veneers inside a frequently used mold is performed by ABAQUS/Explicit and COMSOL software and the results are presented. A multi-factor experimental design methodology is used to analyze computer simulation results in determining the relations between the level of delamination and some of the controllable factors. A multivariate non-linear regression is established based on the results of experimental design and analysis. The regression model can be used to find optimized parameter values in minimizing the level of delamination with significant effects. Numerical examples based on real production settings were used to validate and verify the developed regression model. The solution approach including numerical simulation, experimental design, and non-linear regression can easily be extended for process improvement of similar plywood production systems.

Acknowledgments

First and foremost, I would like to express my deepest appreciation to my supervisor, Dr. Mingyuan Chen for his valuable advice, unparalleled support and profound belief in my abilities and work during my graduate studies. Without his guidance and constant feedback, this degree would not have been achievable. I also appreciate the opportunities were given to me as a research assistant. Warm thanks go to all my friends and officemates at Concordia University: Yasser Ghamary, Walaa Awad Ali, Ruo Liang, César Rodrguez Gallegos, Omar Abuobidalla, Jair Ferrary, Zenan Zhang, Tiansheng Zhang, Dr. Zhifang Zhao, and Alexander Bryce. My success, the completion of my dissertation, would not have been possible without the support and nurturing of my husband, Siamak Arbatani, through the process of researching and writing this thesis. His patience cannot be underestimated. Finally, I would like to express my very sincere gratitude to my parents, Ahmad Zamirian and Zahra Moaddeli, and my brother, Mehrdad Zamirian, for providing me with unconditional support and strong encouragement throughout my years of study.

Contents

List of Figures vii

List of Tables ix

1 Introduction 1

1.1 Introduction to Plywood Manufacturing 2
1.2 Simulation, Modeling, and Optimization 2
1.3 Challenges and Motivation 4
1.4 Contributions 4
1.5 Thesis Outline 5

2 Literature Review 6

2.1 Defects in Plywood Products 6
2.1.1 Types of Defects in Plywood Products 6
2.1.2 Wood Defect Detection and Inspection 10
2.2 Mechanical Properties of Wood and Adhesives 13
2.3 Simulation of Plywood Hot Pressing 16
2.4 Design of Experiment and Optimization 19
2.5 Summary 20

3 Plywood Production 21

3.1 Plywood Production Steps 23
3.1.1 Glue Application 24
3.1.2 Hot Pressing 24
3.2 Defects 27
3.3 Detection of Delamination 32
3.4 Summary 32

4 Simulation and Modeling **33**
4.1 Simulation . . . 33
4.1.1 Modeling Assumptions . . . 34
4.1.2 Numerical Model Parameters of the Hot-Pressing . . . 34
4.1.3 Software and the Modeling Sequence . . . 36
4.1.4 The Structure and Mechanical Behavior of Wood . . . 39
4.1.5 Analysis of Bending with ABAQUS Software . . . 40
4.1.6 Heat Transfer and Moisture Transport Simulation Using COMSOL Software . . . 43
4.1.7 Simulation of the Unloading Step . . . 47
4.1.8 Urea-Formaldehyde based Adhesive . . . 49
4.1.9 Simulation Results . . . 50
4.2 Modeling . . . 53
4.2.1 Factor Effect Estimates . . . 53
4.2.2 Normal Plot of the Effects . . . 57
4.2.3 Half Normal Plot . . . 57
4.2.4 Pareto Chart . . . 58
4.2.5 ANOVA Result . . . 59
4.2.6 Factorial Plots . . . 62
4.2.7 Normal Probability of the Residuals . . . 63
4.2.8 Design Projection . . . 66
4.3 Regression Analysis . . . 68
4.4 Summary . . . 75

5 Conclusion and Future Work **76**
5.1 Conclusion . . . 76
5.2 Future Work . . . 77

Bibliography **84**

Appendices **85**

A Contour, Surface and Cube Plots of Delamination **86**

B MATLAB Code for Parameter Optimization **88**

List of Figures

2.1 Types of delamination: (a) internal delamination (b) near-surface delamination and (c) multiple cracking. 7
2.2 Types of warping defects. 9
3.1 Steps of veneer production and hot pressing. 22
3.2 Heat induction - (a) open mold, (b) closed mold[1]. 25
3.3 Examples of delamination at: (a) edge before sanding, (b) side, (c) edge during sanding, (d) surface before CNC. 29
3.4 Example of twisting. 31
4.1 Hot pressing 3D mold model. 35
4.2 Order of veneers. 36
4.3 Flowchart of the modeling process. 37
4.4 Sequence of hot pressing of veneer sandwich to compute the moisture content. 38
4.5 Sequence of extracting bond strength for glue and unloading step. . . 39
4.6 Radial, longitudinal and tangential directions on orthotropic wood. . 40
4.7 ABAQUS boundary conditions for loading/unloading. 41
4.8 Output of the bending step. Top layer is in long orientation. 42
4.9 Output of the bending step. Top layer is cross oriented. 42
4.10 Surface temperature (K) with all the maximum parameters. 43
4.11 Moisture content (fraction) distribution with all the maximum parameters. 44
4.12 Bonding strength vs moisture content (MC) of PVA adhesive. 47
4.13 Unloaded veneer sandwich with delaminated regions. 48
4.14 Nodal coordinates of first veneer. 49
4.15 Bonding strength vs moisture content (MC) of UF adhesive. 50
4.16 Normal probability plot of the effects. 57

4.17 Half normal plot of the effects. 58
4.18 Pareto chart. 59
4.19 Main effects plot. 62
4.20 Interaction plot. 63
4.21 Normal probability plot of residuals for unrefined model. 64
4.22 Residual versus observation order plot. 64
4.23 Pareto chart of design projection. 67
4.24 Normal probability plot of residuals for refined model. 72
A.1 Contour plots of delamination. 86
A.2 Surface plots of delamination. 87
A.3 Cube plots of delamination. 87

List of Tables

4.1 Factor levels in the pressing process. 35
4.2 The stiffness data used for the studied birch product. 40
4.3 Birch's thermodynamic properties. 43
4.4 Simulation results of moisture content and bonding strength. (part 1) 45
4.5 Simulation results of moisture content and bonding strength. (part 2) 46
4.6 Average delamination in coded parameter space. (part 1) 51
4.7 Average delamination in coded parameter space. (part 2) 52
4.8 Effect estimates.† 56
4.9 ANOVA table, first scenario.† 61
4.10 Unrefined model summary. 65
4.11 ANOVA table, second scenario (design projection).† 68
4.12 ANOVA table for delamination. 70
4.13 Refined model summary. 70
4.14 Variables for the model validation. 73
4.15 Moisture content and bonding strength for the validation scenarios. . 73
4.16 Computed delamination from simulation and refined model. 73

Chapter 1

Introduction

Plywood production is a challenging and complicated process due to the shape stability requirements of the products (Magnevik, 2006). Plywood shape stability means having accurate dimensions and shape of the products within acceptable tolerances throughout the entire manufacturing process in producing high quality plywood products. In this research, the phenomenon of delamination in a certain type of plywood product manufacturing is studied through numerical simulation and the behavior of veneer products exposed to hot-press forming is analyzed. The aim of this research study is to find the root causes of shape instabilities and to obtain optimized parameter values and their combinations for manufacturing process improvement in hot pressing of veneers.

1.1 Introduction to Plywood Manufacturing

Plywood is a building material comprised of veneers glued with an adhesive. Two types of plywood are softwood plywood and hardwood plywood. Softwoods generally correspond to coniferous or evergreen tree species, like firs and pines. Hardwoods, on the other hand, generally correspond to deciduous species, like birch, maple, oak, beech, etc. Hardwood plywood may be formed into panels or plywood components (e.g., curved hardwood plywood, seat backs, chair arms, etc.) by pressing. During the plywood production processes, various types of defects may arise. Delamination between plies, warping, twist, veneer fiber fracture, glue mark, open or closed panel are some of the called veneer defects which may happen during the plywood processing steps from the very first step of plywood production to panel storage. In this research, we focus on delamination defect as the most frequently observed defect.

1.2 Simulation, Modeling, and Optimization

Since quality has different meanings from various aspects, there are several methods to improve it in plywood product manufacturing. Methods such as Six Sigma and lean may reduce manufacturing and quality costs. On the other hand, frameworks like DMAIC (Define, Measure, Analyze, Improve, and Control) can be used in quality-improvement projects. In general, SPC charts, check sheets, scatter plots, cause and effect diagrams, histogram and DOE (DOX) can also be named as quality

improvement tools. Besides the above mentioned experiment-based quality improvement methods and tools, simulation and optimization can be implemented for the purpose of quality improvement (Montgomery, 2012).

In this work, the hot-press step of one of the most frequent molds used in the studied company is simulated by the ABAQUS Finite Element Analysis (FEA) software. The large deformation of the pressing is modeled using the Explicit Dynamic solver. Then the COMSOL Multiphysics® software is used to model the distribution of moisture content under the influence of temperature and pressure in the deformed sandwich. The moisture distribution is used to approximate the bonding strength of glue between the veneers. Finally, the approximated bonding strength of glue is used in the unloading step with ABAQUS software.

The aim of this simulation is to simulate the hot-pressing step with various combinations of parameters in an acceptable margin to correlate the parameters to delamination defect. A design of experiment (DOE) with full factorial design of parameters has been conducted. A mathematical model is created for the studied process. This model is then verified and used for parameter optimization with the goal of minimum delamination defect.

1.3 Challenges and Motivation

Wood is a complex biological material. Moisture exchange between wood and surrounding environment leads to changes on wood performance and mechanical properties. Using wood as an engineering material involves many challenges related to changes in moisture. On the other hand, wood-based composites exhibit anisotropic properties due to its orthotropic mechanical behavior. Commonly observed defects in wood-based products are: delamination between plies, debonding of wood-adhesive layers, wood fiber fracture, warping, crack, glue mark, etc. Among these defects, delamination is the most frequently observed damage, which is defined as separation of two adjacent layers in the laminated wood-based composite (Bucur and Lloyd, 2011).

1.4 Contributions

This research studies the finite element simulation on birch plywood veneers and proposes a mathematical model for delamination defect with respect to controllable effective variables on delamination in the press process in plywood manufacturing. DOE method is used on the obtained results from the simulation. The objectives of obtaining this model are to minimize the delamination defect and to find the best combination of the parameters at their optimum level with the minimum defect. The regression model is tested and validated using numerical examples based on real production settings.

1.5 Thesis Outline

In the following chapter, the literature on this thesis topic is reviewed. In Chapter 3, a brief description of plywood production is given. In Chapter 4, hot pressing of veneer simulation is described, and a mathematical model for minimizing the amount of delamination with respect to the optimum combinations of variables affected in the hot-press is proposed. Finally, the conclusion and future works are presented in Chapter 5.

Chapter 2

Literature Review

A brief review of literature is presented in this chapter on different types of defects in plywood products, defect inspection methods, numerical simulation of the pressing process in plywood production as well as optimization works done in quality improvement and improvements in production systems.

2.1 Defects in Plywood Products

2.1.1 Types of Defects in Plywood Products

In this section, two types of defects, delamination and warping of plywood materials, in plywood manufacturing are discussed.

Delamination

Delamination is the debonding of two adjacent layers in a laminated wood-based composite. This defect is the most commonly observed nonconformity (Bucur and Lloyd, 2011) in plywood product manufacturing. It may result from material defects, improper bonding, detachment of neighboring layers, etc. Depending on the position of the delamination defect in the product, delamination can be categorized as (a) internal crack, (b) near-surface delamination and (c) multiple cracks according to Bolotin (1996). These three types of delamination are schematically shown in Figure 2.1.

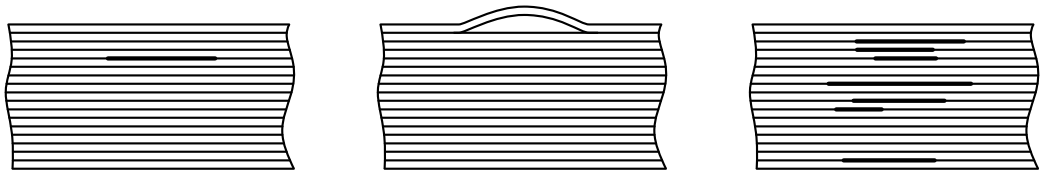

Figure 2.1: Types of delamination: (a) internal delamination (b) near-surface delamination and (c) multiple cracking.

Warping

Many factors can lead to wood warp: air flow, uneven finishing, wood grain direction, temperature and cutting season. In general, the warping defect is related to the wood grain direction. Other factors that can lead to warping are changes in temperature and moisture. According to Hrázskỳ et al. (2011), shape stability of veneers and pressed plywood sheets highly depend on the moisture and temperature. The authors analyzed shape stability of plywood by monitoring the storage of construction veneers, the spread of gluing mixtures, pre-pressing and pressing processes and the

storage of plywood. They also investigated the causes of warping of plywood sheets through laboratory experiments. They concluded that the root causes of warping in plywood sheets is variation of the moisture in veneers, which is also related to temperature. The moisture content of wood and its temperature are related to ambient humidity and temperature as well as pressing parameters, storage and stacking conditions. They related the temperature and moisture parameters to shape and size of camber of the warped veneers.

In terms of mechanical and material properties, unbalanced internal stresses in plywood panels is the root cause of warping (Brouse, 1966). During different stages of plywood production, internal stresses would be reduced if moisture level and moisture distribution are stable in the process of gluing. In fact, construction of plywood is always stressed and the level of warping depends on the balance of the internal stresses of the material.

Warping defects can be categorized as (a) bow (b) cup (c) twist and (d) crook. These defects are schematically shown in Figure 2.2.

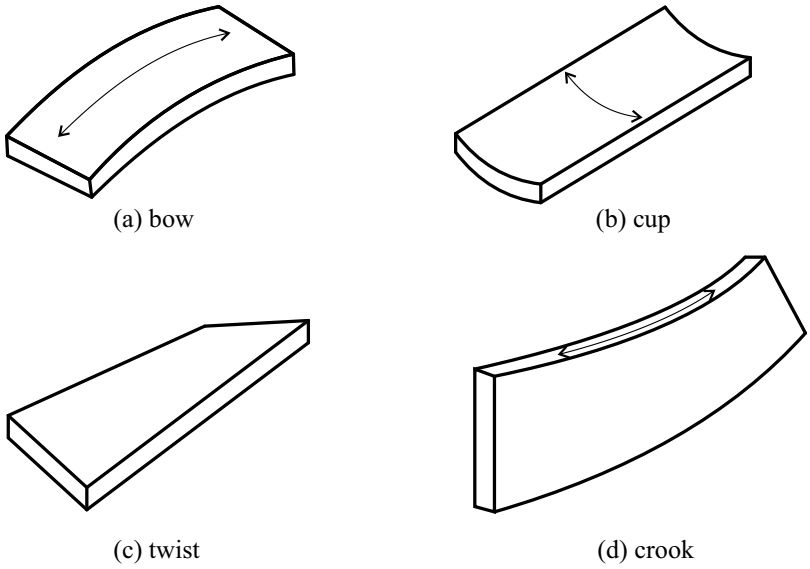

Figure 2.2: Types of warping defects.

A bow is a type of warping defect in a wood-based product that bends along the grain lines. If the board is laid across a flat surface, both ends will be in the air. Cupping occurs when a wooden board bends edge-to-edge across the face. In this case ends of the boards will look like the letter "U". Twist is a general term for a board that bends in any direction and cannot maintain a straight line. A crook or crown is another type of defect found in a board that can be described as end-to-end bent in the direction of the tall ends of a board as it continues down the length of the board[1].

The following factors may contribute to warping[1] (Brouse, 1966):

- Uneven air circulation after peeling the logs results in a bow.
- In thin panels cupping may occur when one face with high moisture content lays on another ply with low moisture content.

[1] `https://www.decks.com/how-to/188/lumber-defects-101`

- Improper handling is another reason for cupping. The plywood should be handled in a way that it absorbs or sends out the moisture equally to prevent any cupping defect. For this purpose, when panels are piled on top of each other, all the edges, ends and top of the plywood must be properly covered.
- When the wood grain direction is not parallel to the edges twist defect may arise. Besides, the clipping and trimming of the veneer should be done parallel to the grain direction. Otherwise, twisting may occur in this situation.
- Uneven drying, before cutting the veneers, may result in a crook defect.

2.1.2 Wood Defect Detection and Inspection

Inspection plays a very important role in quality control and quality improvement throughout the entire production process such as raw materials received from suppliers, during different stages of production and in final product completion and shipment to customers. To detect any defects and those caused by undetected defects in earlier production stages, a set of non-destructive tests are normally conducted and executed.

Several methods of non-destructive tests for plywood products are widely used in the industry. These methods include various visual and mechanical inspections. Visual observations may involve flatness evaluation, crack measurement as well as evaluation of warping and delamination defects. Mechanical inspections may involve moisture and temperature measurements on the materials, production and storage environments along with surface hardness measurement of the material (Delgado et al., 2013).

More advanced inspection techniques are available such as digital image correlation principle as discussed in Burnard et al. (2018) for continuous crack identification and measurements. The authors reported significant reduction in inspection time and increased accuracy of detection.

Other technologies like ultrasonic inspection and proof loading are discussed in Ross et al. (1998). Proof load inspections can be conducted on various pieces of the product and are designed to ensure that the piece being tested is able to tolerate the design load without failure or deformation. Bending, tension and compression are the most commonly used proof loading tests in industry. Ultrasonic inspection in wood composite manufacturing can be used to detect and locate delaminated areas by sending an ultrasonic pulse through the thickness of the panel at each sensor point. The ratio of the magnitude of the transmitted signal to that of the received signal is then used to determine whether a delamination exists.

Near infrared (NIR) technologies have also been widely used in quality control and in sorting products in wood product manufacturing in North America. Near infrared spectroscopy measures the interaction of electromagnetic radiation in the tested materials. Applications of NIR to evaluate chemical, mechanical, and anatomical properties of wood materials are extensive. These techniques are effective in evaluating mechanical properties (strength and stiffness) and some anatomical properties (microfibril angle and fiber diameter) of wood. They can also be used for online characterization of wood composites, such as plywood products. Brashaw et al. (2009)

reviewed NIR techniques used to evaluate the material properties of wood and wood-based products by different companies around the world.

Aderhold and Plinke (2010) and Taylor et al. (2008) used NIR technique to detect wood shrinkage and volumetric swelling. They also estimated wood density using statistical models they developed with a non-linear kernel and wavelet statistical techniques.

Image analyzing techniques along with machine learning methods were presented in Cavalin et al. (2006) for non-destructive detecting of defects in wood materials. The authors used feature extraction from grayscale images to detect defects. They employed neural networks and support vector machines with a feature selection algorithm based on multi-objective genetic algorithms in developing the defect detecting approach. They compared their results with similar techniques using color images.

Another non-conventional non-destructive testing and evaluation technique is infrared thermography. Large surfaces can be rapidly scanned for internal (invisible) defects and structural faults. Thermographic techniques for the identification of defects in wood and lumber are introduced in Aderhold and Plinke (2010) and Meinlschmidt (2005). The authors showed that these methods can be used to mark the delaminated areas or to remove the material completely from the assembly line. They suggested these methods as a possible tool of quality control in wood and lumber manufacturing. Their presented results positively show the possible outlook to introduce these techniques in the field of defect recognition in massive wood surfaces.

Nuclear magnetic resonance (NMR) is also used for non-destructive testing of wood

products. There are a few publications regarding the use of NMR for process monitoring and quality control in the wood-based panel manufacturing (Thoemen, 2010). Potential applications of NMR are the estimation of density, moisture, degree of curing of adhesives and the detection of adhesion defects. NMR can measure these quantities at the same time, giving more accurate and also more stable results.

2.2 Mechanical Properties of Wood and Adhesives

The most vital information needed for an accurate simulation of a plywood molding process is mechanical properties of wood and the adhesive, which is used for bonding of the layers. These properties are the subject of many research works from the early twentieth century so far. Wood is an orthotropic natural material. In that, it is non-homogeneous and the deformation strongly depends on the loading rate. In addition, wood is sensitive to changes in moisture content. All these features make wood a complex material to work with.

In a recent research work, the material properties of medium-density hardwoods are analyzed with the focus on European ash and European beech specimens (Kovryga et al., 2019). They tested the specimens in different loading modes (tension, compression, bending, and shear). They proposed a tensile strength classification system and incorporated their tested total of 3663 specimens in this system.

In another research by Cakiroglu et al. (2019), mechanical properties of birch wood,

one of the most important wood species used in plywood manufacturing, are analyzed along with melamine urea-formaldehyde (MUF) and urea-formaldehyde (UF) glue types in five-ply plywood manufacturing. They compared the results with beech wood.

Moisture content is an intrinsic property of wood. As mentioned earlier, uniform moisture distribution is of importance for service longevity of the final product. Pretreatment methods were investigated to improve uniform evaporation during the hot pressing (Kymäläinen et al., 2018). Incision and cold compression are two of the popular methods for increasing surface exposure and leveling the moisture distribution. Cold compression helps to level the moisture distribution between veneers and therefore helps to avoid imperfect drying and improves overall mechanical properties. This also results in less adhesive consumption up to 20% as well as refined surface characteristics as reported in Bekhta et al. (2009). On the other hand, the incision process helps in uniform evaporation and contributes to increased permeability of adhesive (Kymäläinen et al., 2018).

Mechanical properties of cured wood adhesives are studied in Stoeckel et al. (2013). They recorded measurements of macro and micro-mechanical properties of pure cured adhesive films as well as micro-mechanical characterization of adhesives present in bond lines. The authors drew the following conclusions: (1) Mechanical properties of wood adhesives exhibit a large variability in different conditions. (2) Adhesive formulation, ambient conditions and sample preparation play important roles in the results of measurements of the mechanical properties. (3) The strength of amino

resin based adhesives is higher compared to phenolic adhesives. Isocyanates, epoxy resins and poly vinyl acetate adhesives represent the lowest strength. (4) Moisture usually causes softening in adhesives. Phenolics and structural amino resin show the highest sensibility to moisture content. (5) Stiffness of polyvinyl acetate (PVA), polyurethanes and epoxies decreases with the temperature between the range of 20 to 70 degrees centigrade. Other types of adhesives are less affected to temperature variations.

Authors in Blomqvist et al. (2013) studied distortions in plywood products after molding and during the use. They examined the impact of different UF adhesive systems, adhesive distribution, and veneer properties such as species, moisture level, and fiber orientation. They quantified the distortions right after molding and after exposing the product to changing relative humidity. They concluded that the material and process parameters and the storage in a changing relative humidity had a direct impact on distortion. Differences in moisture content between veneers, fiber orientation, and the moisture gradient in the final product are described in this study as being the most important parameters affecting the distortion and shape stability of plywood products. The reported distortions were relatively small right after the molding. However, the difference in distortions was quite noticeable after exposing the products to changing ambient moisture.

In another work by TenWolde et al. (1988), the effects of moisture, density and temperature on thermal conductivity, thermal diffusivity and specific heat were analyzed

for solid wood. They proposed relationships for approximating these thermal properties with respect to the moisture, density and temperature.

2.3 Simulation of Plywood Hot Pressing

Numerical modeling methods of hot-pressed veneers in plywood processing are studied in this section.

Wood is an orthotropic material and sensitive to loading rate, temperature and moisture content. In veneer molding, the veneer layers are exposed to high temperatures, significant bending, and changes in moisture content due to high temperatures and gluing. These severe conditions may lead to plastic deformations and mechano-sorptive strains in the curved regions. It is difficult to determine the contribution of each parameter to distortions in the veneered product. In general, hot-pressed plywood products are highly sensitive to moisture related distortions. Achieving high quality of veneered products regarding surface appearance, shape stability and rigidity requires improvements in the manufacturing process through a better understanding of the thermo hydro-mechanical behavior of the individual veneers. To study this complicated multi-physics problem which includes temperature, moisture, large deformations, inhomogeneous materials, surface constraints and non-linear glue interaction, finite element-based simulations are proposed and implemented in literature.

In order to simulate large bending deformation of veneers considering high pressure

and temperature along with the effects of moisture content and glue interaction a 3-dimensional finite element model is proposed in Ormarsson and Sandberg (2007). They used ABAQUS software to construct the deformation model and employed ABAQUS subroutines in order to implement the effects of moisture content and glue interaction. The authors showed how stresses, spring-back deformation and moisture related distortions in veneered wood products are influenced by different wood properties and different process parameters.

The thesis work in Magnevik (2006) introduced a finite element model in production chain in manufacturing of a particular chair seat. The author analyzed the forming process using two different finite element (FE) programs. The molding step is done using ABAQUS/Explicit dynamic analysis as a 3D model and the changes in temperature and moisture content are modeled using ABAQUS/Standard solver. Subroutines of the ABAQUS software are used in this work to implement the non-linear behavior of the wood. The author reported a good agreement between the numerical results and the observations made in an industrial setup.

Long term mechanical response of wood under variable humidity and loading conditions is studied with ABAQUS software in Mirianon et al. (2008). The author modeled rheological behavior of wood using ABAQUS subroutines. The moisture distribution is modeled as contributions from moisture flow on the wood surface and moisture diffusion of wood. In several simulations, they demonstrated a good agreement between their implemented model and the experimental results from the literature.

In another work, the problem of progressive failure in plywood material is investigated by Compact Tension (CT) experimental tests and FE analysis. CT specimens of spruce and pine plywood veneers are used in this work. The complicated process of gradual degradation and fracture are modeled as damage growth in plies and delamination of composite layers. The authors used the ABAQUS software to perform numerical simulations and used it for lay-up optimization of the plywood in order to reach higher strength (Ivanov et al., 2008). Although their proposed method is not computationally efficient for large scale simulations, it can be efficiently used for layered composites with delamination.

Radio frequency (RF) or dielectric heating is one of the most commonly used methods of heating in the pressing process of plywood products. Uniform heating plays an important role in the glue curing step of plywood production as the moisture distribution depends directly on the uniformity of the temperature. Therefore, a proper understanding of RF heating on wood-based products is of great importance. Numerical modeling of heat transfer in wood samples by RF heating is studied in Salinas et al. (2017). In this work, the temperature distribution across wood samples was obtained by the integration of the energy equation using the finite volume method. The authors compared the numerical results with experimental data and reported agreement between them.

2.4 Design of Experiment and Optimization

In this section, the recent literature on optimization with the method of design of experiment (DOE) are studied.

Damages in plywood, particularly delamination, are very difficult to model. Therefore, prediction of these damages is a difficult task. Authors in EL Moustaphaoui et al. (2019) employed the DOE to model the delamination damage. They established and analyzed the relationships between the studied parameters and their sources of variation. They used the response surface methodology to quantitatively determine the probability of delamination occurrence as a function of the temperature, pressing time and the amount of glue used in the manufacturing of two types of plywood. Screening study is conducted in this study to demonstrate the non-influential interactions.

The study presented in del Coz Díaz et al. (2013) employed FE method using the ANSYS software to obtain effects of input variables and response surface from DOE analysis for performance of timber joints systems for the beam elements used in the construction of roofs. They were able to improve the manufacturing time, structural fire resistance, faster process of assembly of the roofs element and decrease in the cost of the pieces used.

In another similar study (Lavalette et al., 2016) a full factorial experimental design is implemented to determine the effects of two parameters, the wood moisture content and the amount of adhesive, on the shear strength of softwood plies. Their results

demonstrate optimal results from 30 to 70 percent of moisture content for their studied softwood sample. They concluded that the effect of the amount of adhesive is not significant on the studied range of parameters.

In Buikis et al. (2008) investigation, a mathematical model of the heat and moisture transfer processes for wood like layered materials is proposed. This model is then used to optimize the pressing time and the following cooling time with respect to physical parameters of veneers.

2.5 Summary

In this chapter, literature related to defects, defect detection methods, mechanical properties of wood and adhesives, plywood simulation in the hot pressing process and design of experiment on factors affecting plywood manufacturing were presented. In the next chapter, plywood production is discussed.

Chapter 3

Plywood Production

In this chapter, the process of plywood production is briefly explained. This process is specifically used in a Canadian company based in Montréal in a research collaboration with Concordia University.

The origin of plywood dates back to the ancient Egyptians and Greeks which had an important role in their lives. Nowadays, typical applications of plywood include but not limited to building construction, packaging, transport vehicles, wind turbine blades, furniture, musical instruments[1]. Molded plywood seating production, which is of interest in this thesis work, starts from simple sheets of rotary cut birch. Curved plywood is referred to products used mostly in seats and backs or chairs in a piece of shell. Usually several products are produced in plywood companies like shell, leg, back and seat. The veneers used in this company are hardwood and mostly include birch, beech, maple. Plywood is defined as a material manufactured as veneers ply

[1] https://en.wikipedia.org/wiki/Plywood
www.famitchell.com.au/major-uses-of-plywood

glued to each other. The glued plies are then pressed using a hot-press in order to form the plies and to cure the glue. These steps are schematically shown in Figure 3.1. There are two special types of glues used for this purpose, PVA (Polyvinyl Acetate) and UF (Urea-Formaldehyde). Glue crystallizes as its moisture content reduces. Humidity dissipates from the face of the layers, however, most of it vaporizes by the edges.

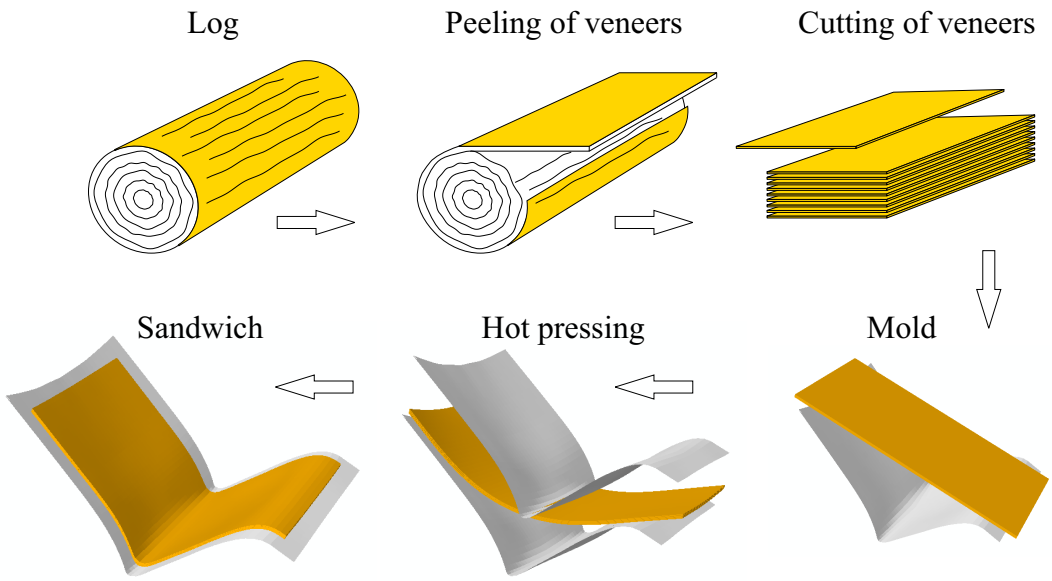

Figure 3.1: Steps of veneer production and hot pressing.

Curing time for PVA is a bit longer than UF. PVA stays flexible for 2-3 hours. A plywood panel based on PVA has more tendency to delaminate and spring back compared to that of UF adhesive used on the same panel. On the other hand, PVA is environment friendly compared to UF adhesive. PVA is single-component and there is no need to mix with other chemical/s which makes it easier to be used. However, PVA is more flexible and prone to softening. However, it should be noted

that glue softening is also a function of time and glue thickness as well as temperature. Finishing operation time is not long enough to raise the temperature and soften the PVA. The general sequence of a completed shell includes gluing, pressing, CNC, sanding, painting (can be optional), and packaging. However, this thesis is mainly focused on gluing and pressing steps. These steps are described in detail in the following. The process in press step commences when the operator sets the specific veneers one at a time on the roller of the glue machine. Based on the instructions of the order, the operator determines which fiber directions of veneers to be used. It is remarkable that the number of sheets is usually odd, so that the sheet is balanced, and it reduces warping. Due to moisture absorption, wood generally expands along its grain. To counter this expansion as well as strengthen the inherent bonding of the layers of wood, they are layered in a crisscross manner so that the grains of each adjacent layer are at right angles and therefore reinforce each others movement along the grains. And since the two outer plies have to usually orient in a certain direction, the total number of plies would be odd. Depending on the type of pressing, Heat Induction (HI) or Radio Frequency (RF), the glue can be PVA or UF.

3.1 Plywood Production Steps

As mentioned above, the general sequence of a completed shell includes gluing, pressing, CNC, sanding, painting (can be optional), and packaging.

3.1.1 Glue Application

The glue is then spread on both sides of the veneer automatically. In the following stage, the operator aligns the layers on top of each other, based on the instructions, cross and long grain.

3.1.2 Hot Pressing

In the next stage, the operator must adjust settings of the press machine with specific features, for instance pressure, cooking time, and temperature in addition to aligning the press machine. Next, he/she cleans the surfaces of the molds by means of air blow gun to prevent any impurity or pollution like chopped wood sticks on the faces of the plywood during the press. As it was mentioned above, HI and RF are the two methods of activating the chemical reaction converting adhesive from liquid to solid.

Heat Induction

In HI, the panel is put in the press. The press is closed, and then the operator turns on the pressure and heating button to start the cooking process. The cooking time varies for different productions, and depends on the type of the wood, the thickness of the panel and design of the mold. The panel is then pressed and heated up in the mold for a certain period namely cooking time. Then the operator opens the mold. Sometimes after cooking time, the hot-pressed veneers are put in cooling jigs to cool down. The cooling jigs must be the shape of the pressing mold, and 4 clamps are attached to the pressed veneers to prevent any potential deformation. This cooling

time (dwell time) may differ for different orders depending on the thickness of the panel sandwich. However, some orders do not need this stage. In the hot-press, the machine must be loaded with veneers as shown in Figure 3.2-a. Then the press closes as shown in Figure 3.2-b. The full pressure is applied to the veneer sandwiches. The operator must set the machine temperature setting to a proper curing temperature. The machine remains at that temperature for specific period of time named curing time until the bonds become strong enough.

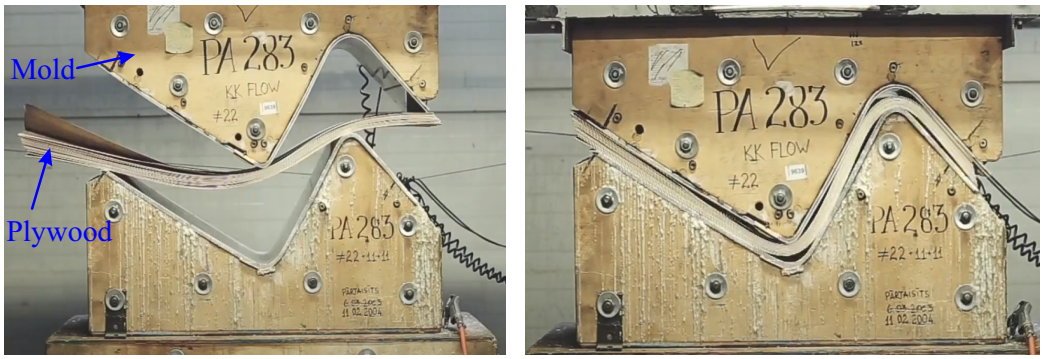

(a) open mold (b) closed mold

Figure 3.2: Heat induction - (a) open mold, (b) closed mold[2].

Radio Frequency Heating

RF heating is the process in which a radio frequency alternating electric field or radio wave heats a dielectric material. This heating is a result of molecular dipole rotation within the dielectric at higher frequencies[3]. One plate is connected to the ground and the other plate is the RF signal. So, the signal travels through the wood vibrates all the molecules of moisture content in the wood. This would lead to heat generation.

[2] www.youtube.com/watch?v=2Vm1yP9UuVA
[3] https://en.wikipedia.org/wiki/Dielectric_heating

This method is based on the same concept as the microwave. The temperature will be the same everywhere in the panel and even in the middle, however, it is difficult to predict where exactly heating starts.

Comparison between HI and RF

As a comparison, it is cheaper to perform the pressing step using the RF because there is no need for heat elements which are used in the HI method. The reason why HI is preferred for the shells in some of the plywood companies is stability in products. HI based heating is uniform due to the equidistant wires inside the plate which results in gradually uniform heating. Also, HI is better for laminates, legs, thin backs and seats and complicated parts where there is a tight radius or something that shape stability is crucial. It is also needed to mention that another reason for the company to use HI for thin products is faster heating step, compared to RF method. In HI method, pressing is much easier since it is not needed that the operator continuously monitors the pressure. The operator just puts the glued veneers in it, and they will not burn compared to the RF method where the inaccurate power adjustment can burn the panel as if the operator sets the device to high power or too much pressing time. These two parameters (power and time) are adjusted by experiment in the RF method.

CNC

After the pressing step, the panels are handled to the CNC department. They are trimmed squared to the desired dimensions by CNC machines.

Sanding of Plywood

Plywood sanding is of importance to remove marks that occurred during the wood-working and also to remove any other flaws like dents which may have appeared while handling it. The sanding operation can be considered as a way of inspection for finished hardwood plywood panel (Schramm, 2003). Prior to sanding, all panels are inspected for mechanical or manufacturing defects. Accuracy of the panel thickness, width, and length in addition to the surface quality are monitored during sanding.

3.2 Defects

Several typical defects might happen during the process of shell production. These defects can be either aesthetic or functional or both. Shell production defects are as follows:

- Aesthetic defects
  - Cigarette Mark: any burning spot during pressing step
  - Dent and Chip: small fragments on wood surface
  - Glue Mark: any remained excessive glue on face or edges
  - Scratches and Wrinkles: any score or mark on the surface

- Functional defects
  - Delamination (discussed earlier)
  - Shrinkage: reduction in dimensions of wood
  - Warping (discussed earlier)
  - Crack: ruptures or separation in the wood grain
  - Open Panel: lower curvature at back and seat of the panel
  - Close Panel: higher curvature at back and seat of the panel

Delamination is a type of defect in plywood when layers are separated in a laminate due to the various reasons such as failure of adhesive, which can happen either at the interface between the wood and adhesive or inside the adhesive itself. There are several factors which can be considered as the major possible causes of this problem. The first reason is the application of insufficient glue on the veneers. The second reason can be a misalignment of the mold that may lead to delamination. Thirdly, insufficient cooking time which leads to uncured glue and separation between the layers as a result.

According to ASTM D 1038, delamination effects in plywood can be described as follows (Bucur and Lloyd, 2011):

- Blister in plywood is bump on the surface due to separation between plies, similar to a blister on the human skin; its boundaries may not be outlined, and it might become flattened or have burst.
- Broken Grain: annual rings might separate on the veneer surface.

- Decrease in durability of the glue bond.
- Gap: a fracture in the inner plies which results when center veneers are broken.
- Open Joint: failure of bond or separation of two adjacent pieces of veneer which leaves an opening, usually happening around the edge joints between veneers.
- Rupturing inside wood which forms various sizes of cavities in radial plane.
- Skips or Voids in the glue line of plywood.
- Starved Joints: a glue joint that is poorly bonded because of an insufficient quantity of glue.
- Sunken joint in plywood: a slight shrinkage at the glue lines.
- Wood Failure either on glue line or wood itself.

Examples of delamination defects are shown in Figure 3.3.

Figure 3.3: Examples of delamination at: (a) edge before sanding, (b) side, (c) edge during sanding, (d) surface before CNC.

Since wood absorbs or loses water, consequently it swells and shrinks. This property

has important practical consequences for the use of wood because variations in ambient relative humidity and temperature during the process, even during the different seasons, resulting in changes in moisture content.

Generally, twisting in plywood is a matter of fiber direction. While other factors rather than grain direction can cause twisting too, they are not so as important as the grain direction. In order to avoid or reduce the twisting that results from grain direction some changes are required in the manufacturing procedure. One of the simplest and inexpensive methods for reducing the twisting is to use odd number of plies and wood types, which generally produce reasonably straight-grained stock. Interlocked and irregularly grained stock should be used where twisting is not a problem (Brouse, 1966). Furthermore, the clipping and trimming of the veneer should be performed parallel to the grain direction.

Twisting is a common type of warpage and cupping which is caused by changes in both moisture and temperature. There are a few potential root causes result in this critical defect that many wood manufacturing industrials may confront. The moisture content is different on the concave side and convex side which results in the warping and bow defect[4]. There will be more warping tendencies by the more severe variations in the moisture content (Brouse, 1966). An example of twisting defect is shown in Figure 3.4.

[4] `http://theplywood.com/flattening-warped`

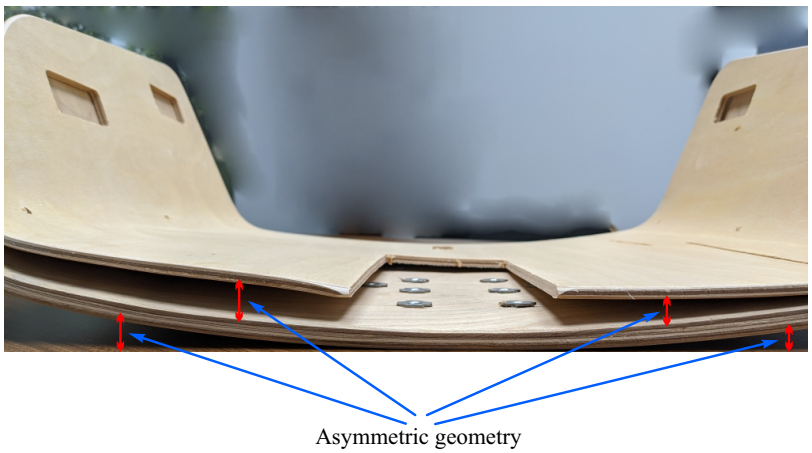

Figure 3.4: Example of twisting.

The next important defect is crack. It is another important cause of a defective shell. This occurs mainly due to the insufficient moisture content in the veneers and high pressure when the mold is not aligned by the operator. In this case, microcracks grow bigger and stress concentration expands to the surface or between the layers.

The wood properties, as well as glue properties, are critical for understanding the material behavior and performance under various operating conditions. Moisture content of 6% to 9% in veneer at the time of hot pressing is satisfactory for hardwood plywood (Vick, 1999). Moisture content (MC) influences delamination of wood cell walls by influencing its ductility (plastic deformation work) (Bucur and Lloyd, 2011). Among other quantities such as strength, stiffness, and dimensional accuracy, the moisture content is an extremely important property of wood, and plywood-based products. For optimum processing conditions in the plywood manufacturing, the moisture variation of veneers should be as low as possible. The moisture content of wood-based panels has to meet a standard value in order to avoid problems like cracks,

twists and other deformations. The lack of reliable, precise, and fast techniques for moisture estimation often causes wood products to fulfill the customers' expectations. Also, reducing the moisture content of veneers to the target value is very energy intensive. A better control of drying process will decrease the energy consumption (Aderhold and Plinke, 2010).

3.3 Detection of Delamination

Although detection of the damage induced by delamination in wood-based composites can be achieved with various methods such as non-destructive ultrasonic methods, in the studied Canadian company, the detection of delamination is only conducted visually. Since it may take 24 hours for the glue to be cured after the pressing, this defect might happen in CNC step (where the stress concentrations are high during the cutting) in the middle of the plywood, while the operator can only investigate the delamination defects near the surface and edges of the plywood.

3.4 Summary

In this chapter, the definition of defects, delamination and warping in particular, and the plywood production processes were presented in detail. As it was discussed, there are plenty of causes leading to delamination defect in plywood production manufacturing. This problem will be simulated in the next chapter and effective factors on delamination will be analyzed.

Chapter 4

Simulation and Modeling

In this chapter, general information regarding wood and its mechanical behavior as well as a brief explanation of plywood production, simulation of veneer hot pressing and modeling and optimization of this process are provided. This approach is applicable to any similar system in plywood manufacturing to study effects of desired factors involved in the process. It should be mentioned that consistency of the results presented in this chapter are verified in a manufacturing setup at the mentioned Canadian company.

4.1 Simulation

This research work is mainly focused on quality improvement in plywood manufacturing. This manufacturing process mainly involves the hot pressing of glued veneers. One of the major defects in hot pressing of veneers is delamination. In this chapter,

a simulation model is presented for the hot pressing. This model allows us to study the large deformation of the veneers during the hot pressing as well as the behavior of the pressed veneer sandwich and bonding strength of the glue. Assumptions as well as input parameters and outputs of this model are explained in the following section.

4.1.1 Modeling Assumptions

Some simplification assumptions are used in this work to make the simulation possible. The temperature as well as the mold pressure in the interface of the plywood sandwich are assumed to be uniformly distributed. Mechanical properties of the wood, like elastic moduli (longitudinal, tangential and radial Young's modulus) and density are assumed to be homogeneous. Veneers are assumed to be initially aligned.

4.1.2 Numerical Model Parameters of the Hot-Pressing

3D model of the mold is provided by a company. This model is based on one of the frequently ordered products. This 3D model is shown in Figure 4.1. Dimensions and the number of veneers are standard for this product. The veneer sandwich is composed of 7 birch veneer sheets of $1/16''$ in thickness, $36''$ in length and $19''$ in width. The lower mold is stationary, and the upper mold is moving with the rate of 50 mm/s. Factor and their levels used in this study are shown in Table 4.1.

Table 4.1: Factor levels in the pressing process.

		Factor Levels	
Factors	Units	Low (-1)	High (+1)
A: Cooking temp., T_c	(K)	365.15	371.15
B: Initial wood moisture, ϕ_w	(%)	6	9
C: Room humidity, ϕ_r	(%)	29	69
D: Room temp., T_r	(K)	297.25	305.35
E: Cooking time, t_c	$(Sec.)$	360	540
F: Mold pressure, P	(atm)	61.24	102.06

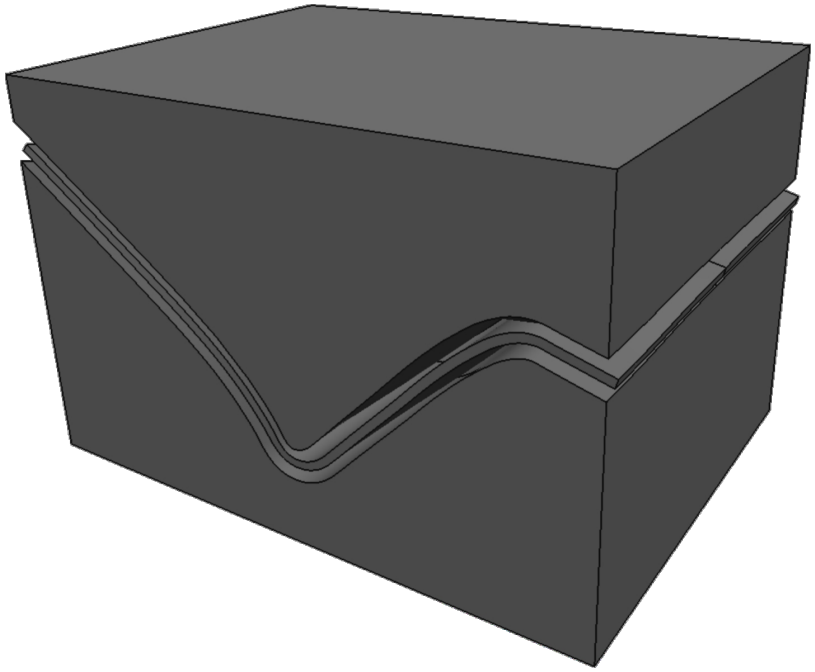

Figure 4.1: Hot pressing 3D mold model.

Order of veneer layers, whether they are long or cross oriented is shown in Figure 4.2.

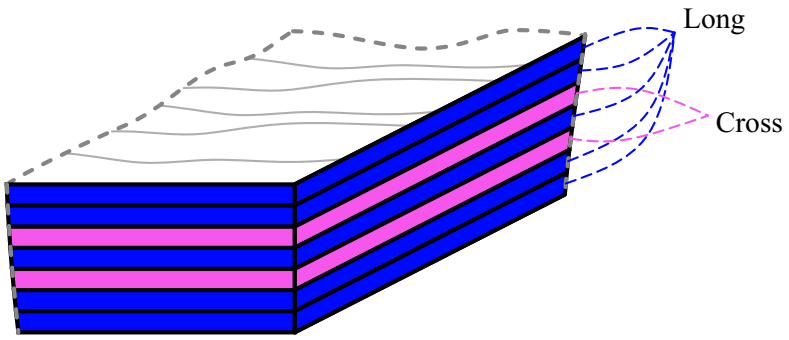

Figure 4.2: Order of veneers.

4.1.3 Software and the Modeling Sequence

Two simulation packages are used in this work to simulate the hot-pressing process of plywood in three steps. First, ABAQUS® software is used to model the pressing step which involves bending the veneer sandwich. Then the COMSOL Multiphysics® is used to model the distribution of moisture content under the influence of temperature and pressure in the deformed sandwich. The moisture distribution is then used to approximate the bonding strength of glue from curves available in the literature. Finally, the approximated bonding strength of glue is used in the unloading step of the ABAQUS model. Flowchart of the entire modeling process is shown in Figure 4.3. The first two steps are schematically shown in Figure 4.4. The third step is shown schematically in Figure 4.5.

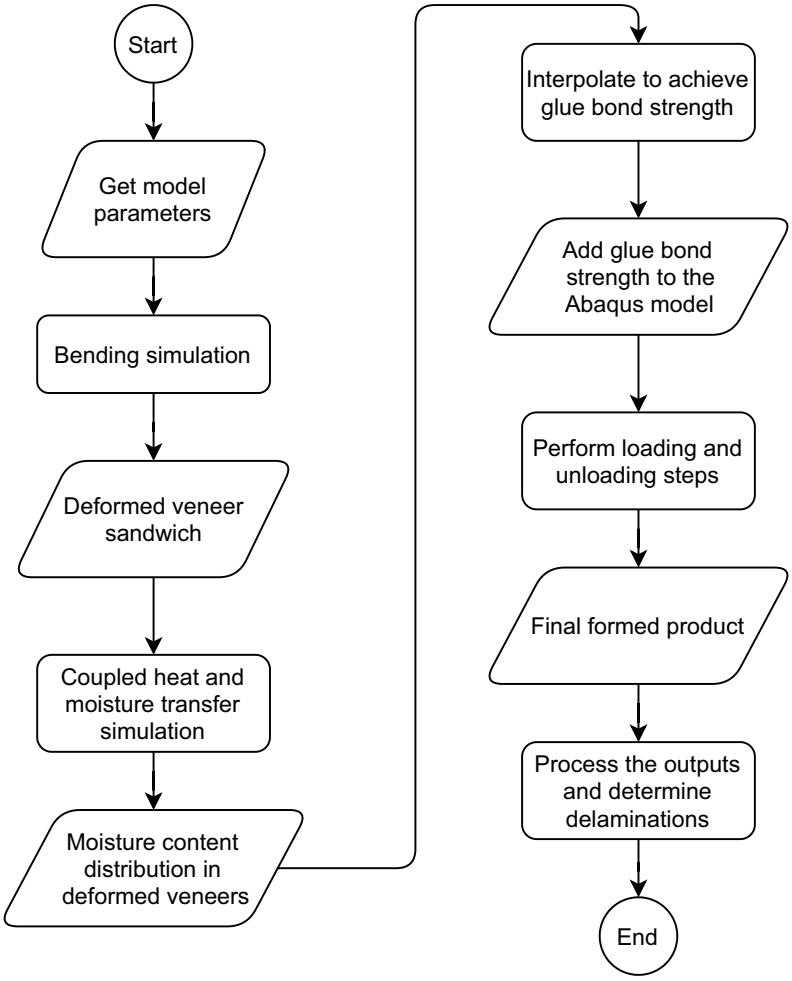

Figure 4.3: Flowchart of the modeling process.

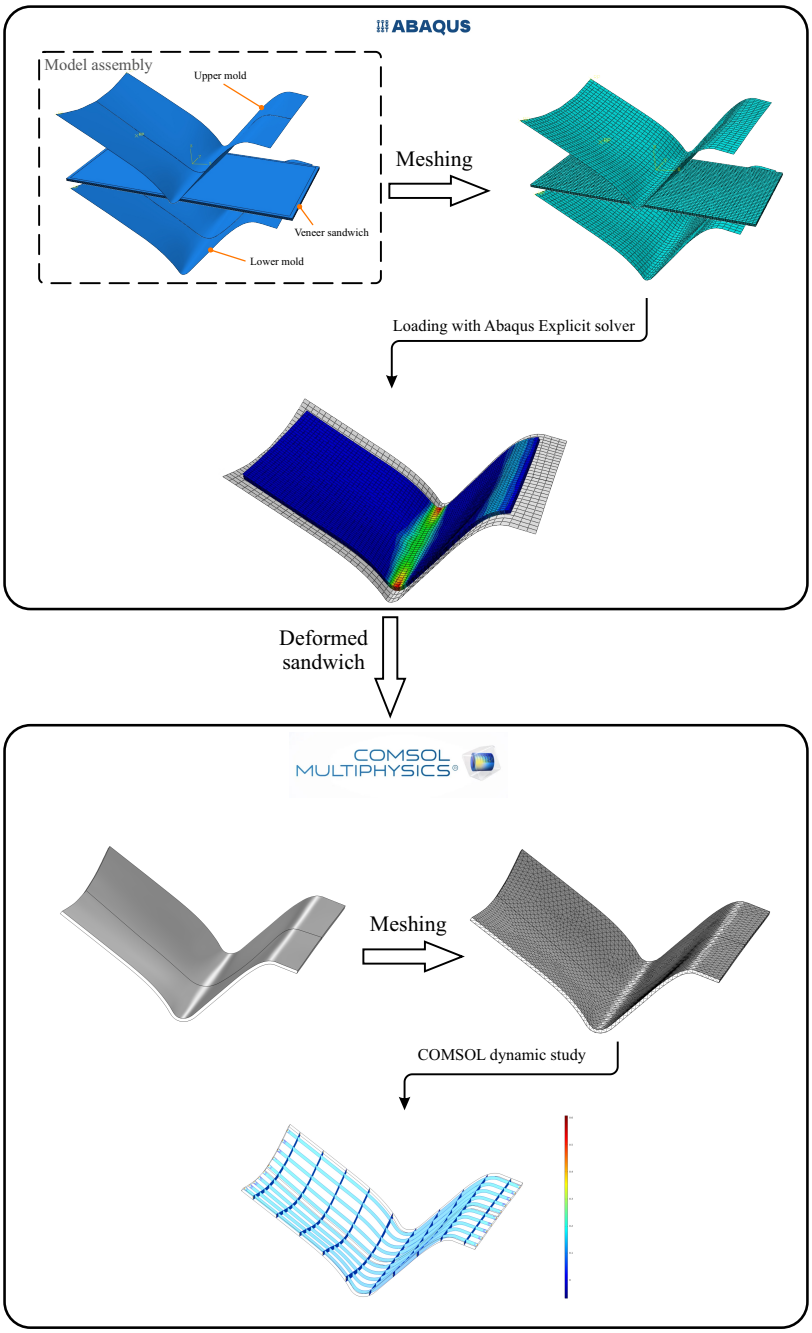

Figure 4.4: Sequence of hot pressing of veneer sandwich to compute the moisture content.

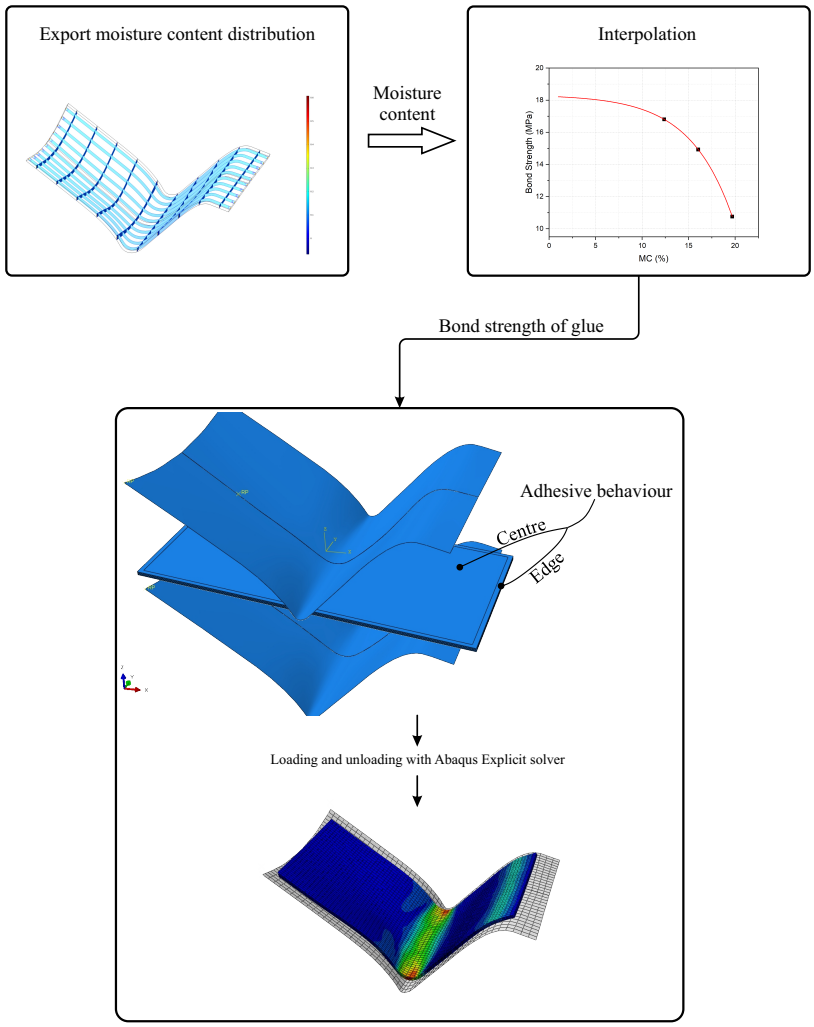

Figure 4.5: Sequence of extracting bond strength for glue and unloading step.

4.1.4 The Structure and Mechanical Behavior of Wood

As mentioned earlier, wood is an orthotropic material which means that materials stiffness properties are different in three principal axes. These three perpendicular directions (radial, longitudinal and tangential directions) are depicted in Figure 4.6. In addition, moisture content and temperature of the wood and the ambient can significantly affect wood behavior. Therefore, deformation of the wood is a highly

non-linear function of loading and ambient conditions. This nonlinearity makes the wood a complex material to model in wood manufacturing.

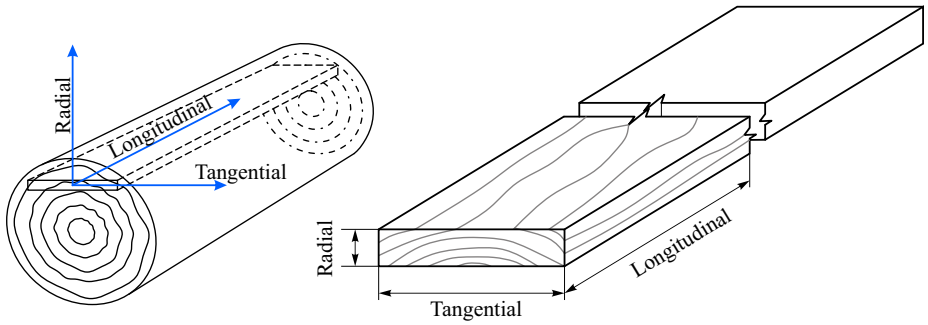

Figure 4.6: Radial, longitudinal and tangential directions on orthotropic wood.

As mentioned, birch veneers are used in this study. Typical orthotropic stiffness parameters for birch veneers are shown in Table 4.2 where E is Young's modulus, G is shear modulus and ν is Poisson's ratio (Ormarsson and Sandberg, 2007).

Table 4.2: The stiffness data used for the studied birch product.

E_l (MPa)	E_r (MPa)	E_t (MPa)	G_{lr} (MPa)	G_{lt} (MPa)	G_{rt} (MPa)	ν_{lr}	ν_{lt}	ν_{rt}
16350	1110	6200	1176	912	186	0.49	0.44	0.72

l: longitudinal, r: radial and t:tangential

These stiffness values along with the birch's mass density, $\rho = 620\ kg/m^3$, are used in the ABAQUS software as material properties for veneers.

4.1.5 Analysis of Bending with ABAQUS Software

Three boundary conditions (BCs) are used in this step:

1. Lower mold part is fixed displacement and rotation BCs.
2. Upper mold part is fixed in all directions except the vertical axis.

3. Upper mold is moving with a constant rate of $V_z = -50\ mm/s$ using velocity BC in the vertical direction.

These BCs are shown in Figure 4.7.

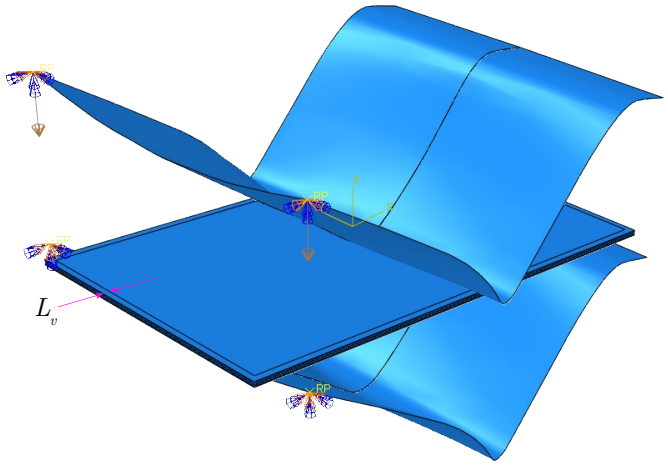

Figure 4.7: ABAQUS boundary conditions for loading/unloading.

The interaction between the mold surfaces with upper and lower veneer as well as the interaction between the veneer surfaces are modeled using the penalty contact method. Hard contact is used as the normal contact behavior and friction coefficient of $\mu = 0.05$ (Magnevik, 2006) is used in this model as tangential contact behavior. The bending step is done for $t_l = 5.7\ Sec.$ using the ABAQUS Explicit solver. The mass scaling factor of 500 used in this step to speed up the simulation as the step is not involving any fast-moving object or impact.

The deformed geometry output of this step is shown in Figure 4.8. Von-Mises stress values are presented with a color gradient in this figure. Note that the shown top layer in this figure is in long orientation, according to Figure 4.2. The stress concentration

regions which are potential failure points are visually distinguishable in this figure. Similar results of deformation for the third layer from the top, which is in cross orientation is shown in Figure 4.9.

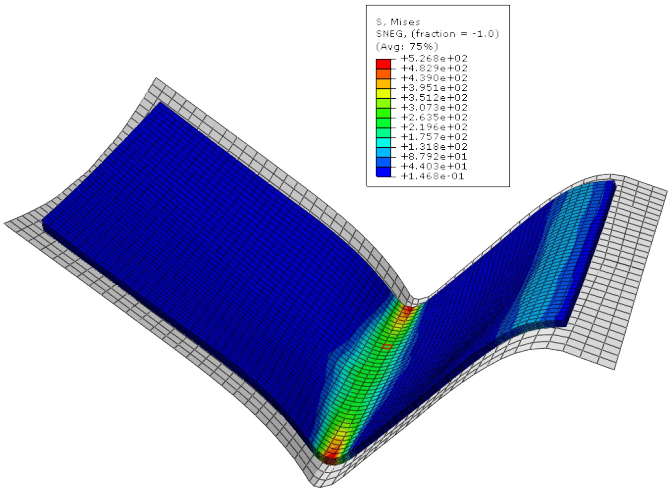

Figure 4.8: Output of the bending step. Top layer is in long orientation.

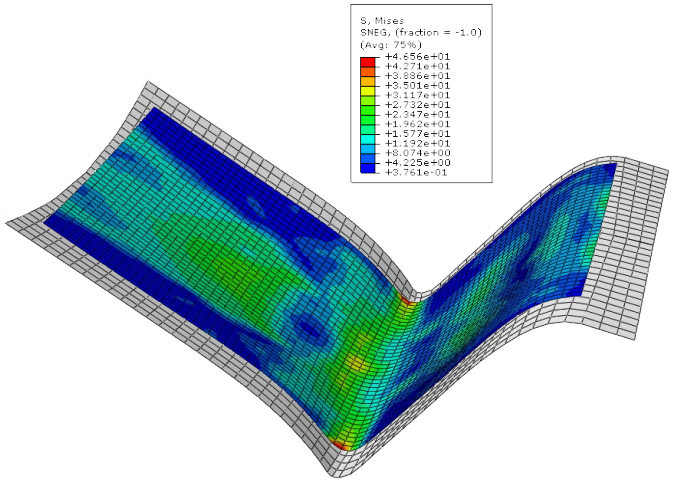

Figure 4.9: Output of the bending step. Top layer is cross oriented.

4.1.6 Heat Transfer and Moisture Transport Simulation Using COMSOL Software

The deformed geometry from the output of ABAQUS's bending step is imported to the COMSOL software. Coupled heat transfer and moisture transport modules are used to model these two phenomena in the deformed veneer sandwich. Birch's thermodynamic material properties used in this analysis are shown in Table 4.3.

Table 4.3: Birch's thermodynamic properties.

ρ (Kg/m^3)	C_p $(J/(KgK))$	λ $(W/(mK))$	D $(m^2/Sec.)$
520	390	0.173	3.3×10^{-10}

In this table, ρ is mass density, C_p is heat capacity, λ is thermal conductivity and D is diffusion coefficient. According to Table 4.1, 64 number of simulations are performed with all the combinations of maximum and minimum values of the hot pressing parameters. Examples of surface temperature and moisture content distribution are shown in Figure 4.10 and Figure 4.11 for the case of all maximum parameters.

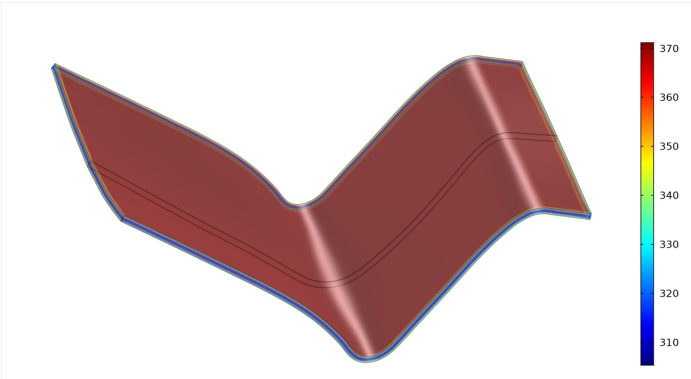

Figure 4.10: Surface temperature (K) with all the maximum parameters.

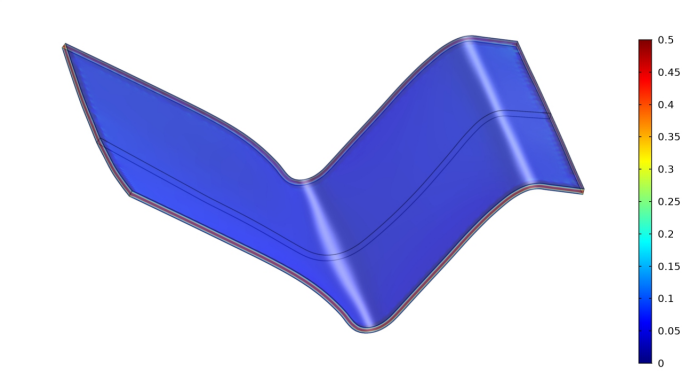

Figure 4.11: Moisture content (fraction) distribution with all the maximum parameters.

The results show that the variation of moisture content is almost only at the edges of the deformed veneer sandwich. The length of this region is measured in all the simulation outputs and found to be $L_v = 12.5 \pm 0.25\ mm$. In order to simplify the modeling process of the following steps, two values of moisture content are assigned to each model:

1. The moisture content of the edge (the region from the edge of the veneer sandwich up to the depth of L_v). This region is shown in the FEM assembly of Figure 4.7.
2. The moisture content of the center region.

Simulation results of the all the 64 configurations are shown in two parts in Table 4.4 and Table 4.5. The data shown in these tables are as follows:

- T_c: Cooking temperature
- ϕ_w: Initial wood moisture
- ϕ_r: Room humidity
- T_r: Room temperature
- t_c: Cooking time

- P: Mold pressure
- ϕ_e: Moisture content at the edge after cooking
- ϕ_c: Moisture content at the center region after cooking
- σ_e: Bonding strength of glue at the edge
- σ_c: Bonding strength of glue at the center region

Table 4.4: Simulation results of moisture content and bonding strength. (part 1)

No.	T_c (K)	ϕ_w (%)	ϕ_r (%)	T_r (K)	t_c $(Sec.)$	P (atm)	ϕ_e (%)	ϕ_c (%)	σ_e (MPa)	σ_c (MPa)
1	365.15	6	29	297.25	360	61.24	5.01	3.71	20.6088	21.2686
2	371.15	6	29	297.25	360	61.24	3.75	2.28	21.2483	21.9944
3	365.15	9	29	297.25	360	61.24	4.78	3.82	20.7255	21.2128
4	371.15	9	29	297.25	360	61.24	3.73	2.26	21.2585	22.0046
5	365.15	6	69	297.25	360	61.24	11.7	9.76	17.2132	18.1979
6	371.15	6	69	297.25	360	61.24	8.46	6.81	18.8577	19.6952
7	365.15	9	69	297.25	360	61.24	12.15	9.03	16.9848	18.5684
8	371.15	9	69	297.25	360	61.24	9.11	7.12	18.5278	19.5378
9	365.15	6	29	305.35	360	61.24	5.91	4.35	20.152	20.9438
10	371.15	6	29	305.35	360	61.24	4.26	3.00	20.9894	21.629
11	365.15	9	29	305.35	360	61.24	6.22	4.82	19.9946	20.7052
12	371.15	9	29	305.35	360	61.24	4.7	2.92	20.7661	21.6696
13	365.15	6	69	305.35	360	61.24	13.35	10.06	16.3757	18.0456
14	371.15	6	69	305.35	360	61.24	10.49	7.5	17.8274	19.345
15	365.15	9	69	305.35	360	61.24	12.51	11.46	16.8021	17.335
16	371.15	9	69	305.35	360	61.24	10.72	7.93	17.7106	19.1267
17	365.15	6	29	297.25	540	61.24	5.05	4.02	20.5885	21.1113
18	371.15	6	29	297.25	540	61.24	3.65	2.47	21.2991	21.898
19	365.15	9	29	297.25	540	61.24	4.9	3.63	20.6646	21.3092
20	371.15	9	29	297.25	540	61.24	3.74	2.57	21.2534	21.8472
21	365.15	6	69	297.25	540	61.24	12.46	9.91	16.8275	18.1217
22	371.15	6	69	297.25	540	61.24	9.92	7.13	18.1167	19.5328
23	365.15	9	69	297.25	540	61.24	11.42	8.89	17.3553	18.6394
24	371.15	9	69	297.25	540	61.24	8.46	6.72	18.8577	19.7409
25	365.15	6	29	305.35	540	61.24	5.93	4.98	20.1418	20.624
26	371.15	6	29	305.35	540	61.24	4.87	2.92	20.6798	21.6696
27	365.15	9	29	305.35	540	61.24	5.75	4.36	20.2332	20.9387
28	371.15	9	29	305.35	540	61.24	4.77	2.88	20.7306	21.6899
29	365.15	6	69	305.35	540	61.24	13.34	10.08	16.3808	18.0355
30	371.15	6	69	305.35	540	61.24	11.13	7.53	17.5025	19.3297
31	365.15	9	69	305.35	540	61.24	13.09	10.25	16.5077	17.9492
32	371.15	9	69	305.35	540	61.24	10.59	7.88	17.7766	19.1521

Table 4.5: Simulation results of moisture content and bonding strength. (part 2)

No.	T_c (K)	ϕ_w (%)	ϕ_r (%)	T_r (K)	t_c $(Sec.)$	P (atm)	ϕ_e (%)	ϕ_c (%)	σ_e (MPa)	σ_c (MPa)
33	365.15	6	29	297.25	360	102.07	5.87	4.76	20.1723	20.7357
34	371.15	6	29	297.25	360	102.07	4.19	2.78	21.025	21.7406
35	365.15	9	29	297.25	360	102.07	5.9	4.67	20.1571	20.7813
36	371.15	9	29	297.25	360	102.07	4.44	2.67	20.8981	21.7965
37	365.15	6	69	297.25	360	102.07	13.74	10.49	16.1778	17.8274
38	371.15	6	69	297.25	360	102.07	11.18	8.17	17.4771	19.0049
39	365.15	9	69	297.25	360	102.07	13.88	10.75	16.1067	17.6954
40	371.15	9	69	297.25	360	102.07	10.13	7.94	18.0101	19.1216
41	365.15	6	29	305.35	360	102.07	6.39	5.05	19.9083	20.5885
42	371.15	6	29	305.35	360	102.07	5.53	3.59	20.3448	21.3295
43	365.15	9	29	305.35	360	102.07	6.43	5.11	19.888	20.558
44	371.15	9	29	305.35	360	102.07	5.02	3.33	20.6037	21.4615
45	365.15	6	69	305.35	360	102.07	16.27	13.2	14.8937	16.4519
46	371.15	6	69	305.35	360	102.07	11.94	8.66	17.0914	18.7562
47	365.15	9	69	305.35	360	102.07	16.08	12.64	14.9901	16.7361
48	371.15	9	69	305.35	360	102.07	11.77	8.78	17.1777	18.6953
49	365.15	6	29	297.25	540	102.07	6.06	4.52	20.0758	20.8575
50	371.15	6	29	297.25	540	102.07	4.29	2.9	20.9742	21.6797
51	365.15	9	29	297.25	540	102.07	5.5	4.78	20.3601	20.7255
52	371.15	9	29	297.25	540	102.07	4.04	2.74	21.1011	21.7609
53	365.15	6	69	297.25	540	102.07	14.2	11.02	15.9443	17.5583
54	371.15	6	69	297.25	540	102.07	10.15	7.33	17.9999	19.4312
55	365.15	9	69	297.25	540	102.07	13.1	11.08	16.5026	17.5279
56	371.15	9	69	297.25	540	102.07	10.68	7.55	17.7309	19.3196
57	365.15	6	29	305.35	540	102.07	6.41	5.04	19.8982	20.5936
58	371.15	6	29	305.35	540	102.07	4.91	3.4	20.6595	21.426
59	365.15	9	29	305.35	540	102.07	6.5	5.48	19.8525	20.3702
60	371.15	9	29	305.35	540	102.07	5.6	3.57	20.3093	21.3397
61	365.15	6	69	305.35	540	102.07	15.56	11.61	15.254	17.2589
62	371.15	6	69	305.35	540	102.07	11.78	9.2	17.1726	18.4821
63	365.15	9	69	305.35	540	102.07	16.51	11.51	14.7718	17.3096
64	371.15	9	69	305.35	540	102.07	12.69	8.74	16.7107	18.7156

The bonding strength values are derived by linear regression and extrapolation from the data presented in (Bomba et al., 2014). The data points and linear regression are shown in Figure 4.12.

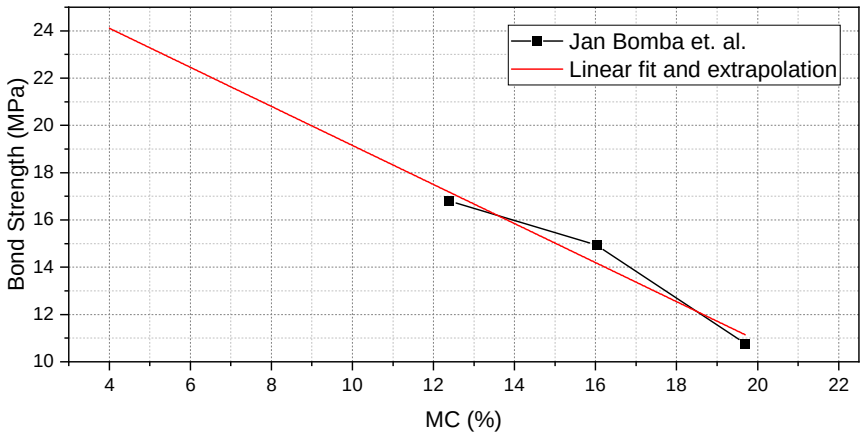

Figure 4.12: Bonding strength vs moisture content (MC) of PVA adhesive.

4.1.7 Simulation of the Unloading Step

Once the bonding strength of glue achieved from the coupled simulation of heat transfer and moisture transport, the unloading step is simulated in ABAQUS software. For this step, the adhesive contact behavior is defined between the veneers and the bonding strength values from previous calculations (Tables 4.4 and 4.5) are used as the adhesive properties. Boundary conditions in this step are similar to the ones in the loading step with a vertical displacement rate of $V_z = 50\ mm/Sec.$. The duration of this step is $t_u = 4\ Sec.$. And unloaded veneer sandwich is shown in Figure 4.13. Two delamination regions are shown in this figure.

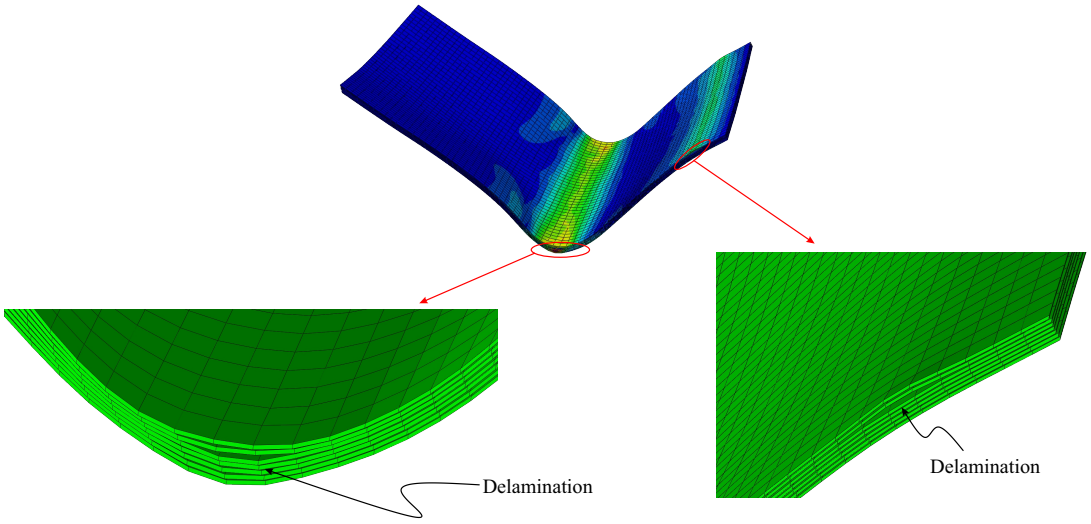

Figure 4.13: Unloaded veneer sandwich with delaminated regions.

In order to measure and compare the delamination in all the 64 simulation cases, coordinates of all the nodal points of each layer in each case are extracted. An example of nodal coordinates is plotted for the first layer in Figure 4.14. The average distance between the layers, θ, are computed using Eq. 4.1. In this equation, m is the number of the veneer sheets and n is the number of the nodes per veneer sheet in the FEM model.

$$\theta = \frac{\sum_{i=1}^{m-1} \sum_{j=1}^{n} \sqrt{\left(x_{ij} - x_{(i+1)j}\right)^2 + \left(y_{ij} - y_{(i+1)j}\right)^2 + \left(z_{ij} - z_{(i+1)j}\right)^2}}{(m-1)\, n} \tag{4.1}$$

where x_{ij}, y_{ij} and z_{ij} are coordinates of node i along global x, y and z axes in layer j. In this work, $m = 7$ and $n = 2960$.

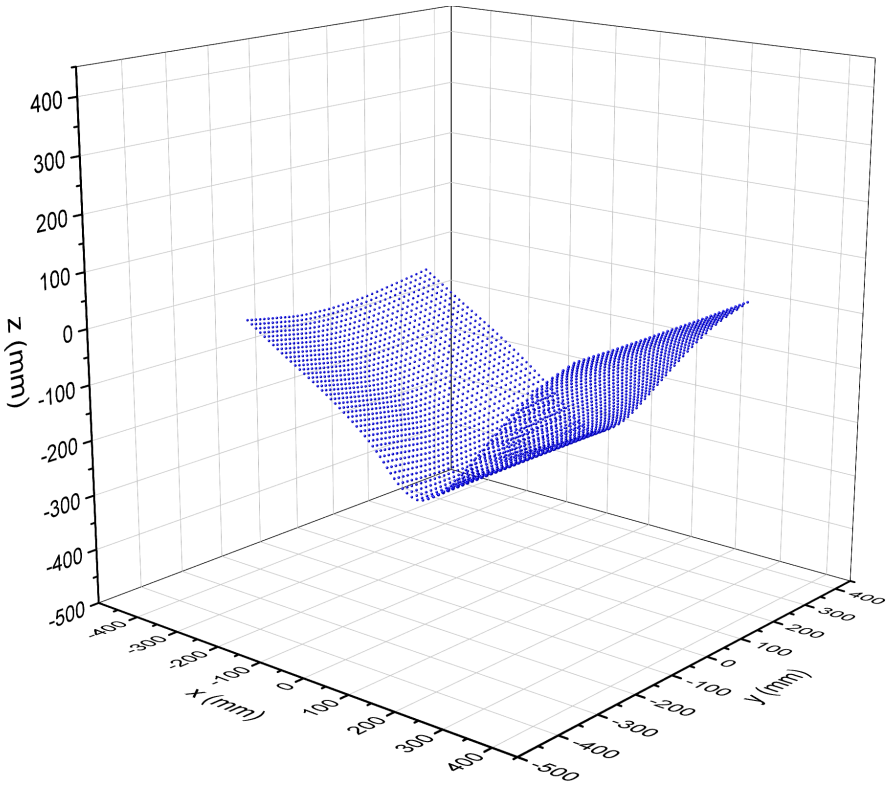

Figure 4.14: Nodal coordinates of first veneer.

4.1.8 Urea-Formaldehyde based Adhesive

According to the experimental data from (Bardak et al., 2018) shown in Figure 4.15, the bonding strength of UF adhesive is not affected by moisture content. Therefore, the parameter optimization of the hot pressing process with the UF adhesive is not plausible.

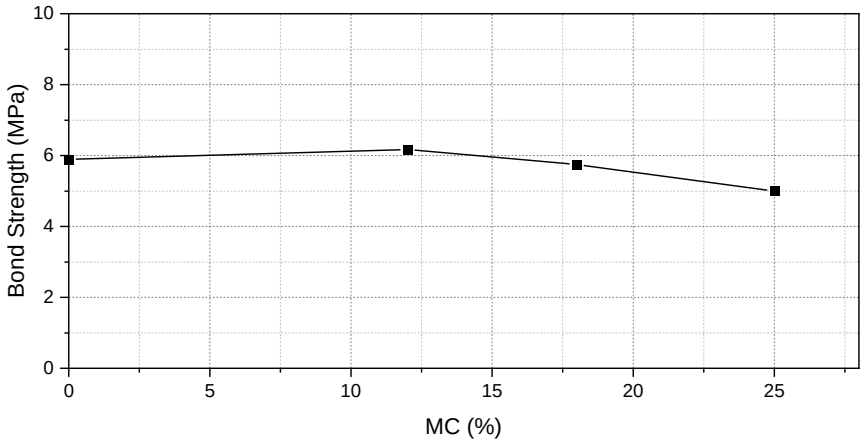

Figure 4.15: Bonding strength vs moisture content (MC) of UF adhesive.

4.1.9 Simulation Results

Results of simulation with coded parameters are shown in Table 4.6 and Table 4.7.

Table 4.6: Average delamination in coded parameter space. (part 1)

	T_c	ϕ_w	ϕ_r	T_r	t_c	P	
Std. order	A	B	C	D	E	F	θ
1	-1	-1	-1	-1	-1	-1	0.055
2	1	-1	-1	-1	-1	-1	0.0538
3	-1	1	-1	-1	-1	-1	0.0545
4	1	1	-1	-1	-1	-1	0.054
5	-1	-1	1	-1	-1	-1	0.0619
6	1	-1	1	-1	-1	-1	0.059
7	-1	1	1	-1	-1	-1	0.061
8	1	1	1	-1	-1	-1	0.0577
9	-1	-1	-1	1	-1	-1	0.0547
10	1	-1	-1	1	-1	-1	0.0546
11	-1	1	-1	1	-1	-1	0.0542
12	1	1	-1	1	-1	-1	0.0545
13	-1	-1	1	1	-1	-1	0.0631
14	1	-1	1	1	-1	-1	0.059
15	-1	1	1	1	-1	-1	0.0742
16	1	1	1	1	-1	-1	0.0581
17	-1	-1	-1	-1	1	-1	0.0552
18	1	-1	-1	-1	1	-1	0.0539
19	-1	1	-1	-1	1	-1	0.0547
20	1	1	-1	-1	1	-1	0.0543
21	-1	-1	1	-1	1	-1	0.0624
22	1	-1	1	-1	1	-1	0.0586
23	-1	1	1	-1	1	-1	0.0606
24	1	1	1	-1	1	-1	0.0582
25	-1	-1	-1	1	1	-1	0.0545
26	1	-1	-1	1	1	-1	0.0547
27	-1	1	-1	1	1	-1	0.054
28	1	1	-1	1	1	-1	0.0545
29	-1	-1	1	1	1	-1	0.0625
30	1	-1	1	1	1	-1	0.0589
31	-1	1	1	1	1	-1	0.0751
32	1	1	1	1	1	-1	0.0583

Table 4.7: Average delamination in coded parameter space. (part 2)

	T_c	ϕ_w	ϕ_r	T_r	t_c	P	
Std. order	A	B	C	D	E	F	θ
33	-1	-1	-1	-1	-1	1	0.0545
34	1	-1	-1	-1	-1	1	0.0535
35	-1	1	-1	-1	-1	1	0.0543
36	1	1	-1	-1	-1	1	0.0539
37	-1	-1	1	-1	-1	1	0.0609
38	1	-1	1	-1	-1	1	0.0584
39	-1	1	1	-1	-1	1	0.0605
40	1	1	1	-1	-1	1	0.0574
41	-1	-1	-1	1	-1	1	0.0543
42	1	-1	-1	1	-1	1	0.0542
43	-1	1	-1	1	-1	1	0.0537
44	1	1	-1	1	-1	1	0.0541
45	-1	-1	1	1	-1	1	0.0616
46	1	-1	1	1	-1	1	0.0585
47	-1	1	1	1	-1	1	0.0736
48	1	1	1	1	-1	1	0.0572
49	-1	-1	-1	-1	1	1	0.0548
50	1	-1	-1	-1	1	1	0.0536
51	-1	1	-1	-1	1	1	0.0541
52	1	1	-1	-1	1	1	0.054
53	-1	-1	1	-1	1	1	0.0613
54	1	-1	1	-1	1	1	0.0578
55	-1	1	1	-1	1	1	0.0603
56	1	1	1	-1	1	1	0.0575
57	-1	-1	-1	1	1	1	0.0542
58	1	-1	-1	1	1	1	0.0543
59	-1	1	-1	1	1	1	0.054
60	1	1	-1	1	1	1	0.054
61	-1	-1	1	1	1	1	0.0621
62	1	-1	1	1	1	1	0.0586
63	-1	1	1	1	1	1	0.0724
64	1	1	1	1	1	1	0.0577

where T_c is cooking temperature, ϕ_w is initial moisture content of wood, ϕ_r is room humidity, T_r is room temperature, t_c is cooking time and P is mold pressure.

4.2 Modeling

In this section, the controllable variables affecting the pressing step and the effect of each parameter and their interactions between them are analyzed using Minitab 18 software. According to that, a mathematical model is provided which relates these variables to the amount of delamination defect in the pressing step. Next, the amount of delamination is minimized using this mathematical model. For this purpose, as mentioned in Section 4.1.2, there are 6 factors, cooking temperature, initial moisture content of wood, room humidity, room temperature, cooking time, and mold pressure, each at two levels of maximum and minimum as shown in Table 4.1. The methodology of this analysis is explained in (Box et al., 2005) and (Montgomery, 2013, chapters. 5 and 6).

4.2.1 Factor Effect Estimates

Analysis results show that factors and their interactions have both positive and negative impacts on the amount of delamination. In two levels factorial design experiments, it is important to investigate the magnitude and direction of the effect of each factor to determine which factors and their interactions are potentially important. The table of main effects and interaction effects estimations are obtained using the Minitab software and shown in Table 4.8. This factorial design analysis includes terms in the model up through order 4.

Effect estimates

It is the magnitude of the factors affecting the response variable. It is calculated as follows:

$$\textit{Effect estimate} = \frac{\sum(\text{response factor at high level})}{n_{\text{response factor at high level}}} - \frac{\sum(\text{response factor at low level})}{n_{\text{response factor at low level}}} \tag{4.2}$$

Coefficient

It is the half of the effect estimate that is used in the regression equation as a coefficient:

$$\textit{Coefficient} = \frac{\textit{Effect estimate}}{2} \tag{4.3}$$

SE coefficient

It stands for the standard error of the coefficient that measures the accuracy of the estimate of the coefficient. The smaller the standard error, the more precise the estimate. *SE coefficient* in Table 4.8 is equal to 0.00005 for all the effects.

P-value

In this table, the factors which have the *P-value* less than the significance level ($\alpha = 0.05$) are considered as significant factors, having an impact on the result, and the factors with *P-value* higher than 0.05 are insignificant.

To give an example, the *P-value* of the interaction CF is 0.058 is bigger than 0.05, so it is insignificant (Louvet and Delplanque, 2005).

VIF

VIF in ANOVA table stands for variance inflation factors which is another method for describing how much correlation exists between the predictors in a regression analysis. Correlation between the predictors is problematic because it can increase the variance of the regression coefficients, making it difficult to judge the individual impact that each of the correlated predictors has on the response. The common measures for *VIF* are as follows:

$$\text{Status of predictors:} \begin{cases} VIF = 1 \Rightarrow \text{Not correlated} \\ 1 < VIF < 5 \Rightarrow \text{Moderately correlated} \\ VIF > 5 \Rightarrow \text{Highly correlated} \end{cases} \tag{4.4}$$

Thus, the *VIF* value of 1 means that the predictor is not correlated with other variables. As it can be seen, all the *VIF* values in Table 4.8 are equal to 1. To give an instance, consider the interaction AB effect, interaction between the cooking temperature and the initial moisture content of the wood. The *VIF* value of AB is 1. It means that the initial moisture content of the wood, when the wood is not yet in the press, is independent from the cooking temperature. And the cooking temperature does not affect the initial moisture content of the wood. In fact, the cooking temperature only affects the final moisture content.

Table 4.8: Effect estimates.[†]

Term	*Effect*	*Coef*	*T-Value*	*P-Value*	*VIF*	
Constant		0.057828	1166.7	0		
A	-0.003356	-0.001678	-33.86	0	1	Significant
B	0.001006	0.000503	10.15	0	1	Significant
C	0.007119	0.003559	71.81	0	1	Significant
D	0.001806	0.000903	18.22	0	1	Significant
E	0.000038	0.000019	0.38	0.716	1	Not significant
F	-0.000575	-0.000287	-5.8	0.001	1	Significant
A*B	-0.001381	-0.000691	-13.93	0	1	Significant
A*C	-0.003056	-0.001528	-30.83	0	1	Significant
A*D	-0.001456	-0.000728	-14.69	0	1	Significant
A*E	0.000025	0.000012	0.25	0.808	1	Not significant
A*F	0.000113	0.000056	1.13	0.294	1	Not significant
B*C	0.001194	0.000597	12.04	0	1	Significant
B*D	0.001481	0.000741	14.94	0	1	Significant
B*E	0.000013	0.000006	0.13	0.903	1	Not significant
B*F	0	0	0	1	1	Not significant
C*D	0.001781	0.000891	17.97	0	1	Significant
C*E	-0.000025	-0.000012	-0.25	0.808	1	Not significant
C*F	-0.000225	-0.000112	-2.27	0.058	1	Not significant
D*E	-0.000025	-0.000013	-0.25	0.808	1	Not significant
D*F	-0.000075	-0.000037	-0.76	0.474	1	Not significant
E*F	-0.000031	-0.000016	-0.32	0.762	1	Not significant
A*B*C	-0.001656	-0.000828	-16.71	0	1	Significant
A*B*D	-0.001656	-0.000828	-16.71	0	1	Significant
A*B*E	0.000125	0.000062	1.26	0.248	1	Not significant
A*B*F	-0.000013	-0.000006	-0.13	0.903	1	Not significant
A*C*D	-0.001919	-0.000959	-19.36	0	1	Significant
A*C*E	0	0	0	1	1	Not significant
A*C*F	0.0001	0.00005	1.01	0.347	1	Not significant
A*D*E	0.000062	0.000031	0.63	0.548	1	Not significant
A*D*F	0.000038	0.000019	0.38	0.716	1	Not significant
A*E*F	0.000006	0.000003	0.06	0.951	1	Not significant
B*C*D	0.001606	0.000803	16.2	0	1	Significant
B*C*E	0.000025	0.000013	0.25	0.808	1	Not significant
B*C*F	-0.000025	-0.000013	-0.25	0.808	1	Not significant
B*D*E	0.000025	0.000013	0.25	0.808	1	Not significant
B*D*F	-0.000125	-0.000062	-1.26	0.248	1	Not significant
B*E*F	-0.000106	-0.000053	-1.07	0.319	1	Not significant
C*D*E	0.00005	0.000025	0.5	0.629	1	Not significant
C*D*F	-0.000063	-0.000031	-0.63	0.548	1	Not significant
C*E*F	-0.000031	-0.000016	-0.32	0.762	1	Not significant
D*E*F	0.000031	0.000016	0.32	0.762	1	Not significant
A*B*C*D	-0.001519	-0.000759	-15.32	0	1	Significant
A*B*C*E	0.000125	0.000062	1.26	0.248	1	Not significant
A*B*C*F	0	0	0	1	1	Not significant
A*B*D*E	-0.000113	-0.000056	-1.13	0.294	1	Not significant
A*B*D*F	0.000037	0.000019	0.38	0.716	1	Not significant
A*B*E*F	0.000081	0.000041	0.82	0.439	1	Not significant
A*C*D*E	0.00005	0.000025	0.5	0.629	1	Not significant
A*C*D*F	0.000113	0.000056	1.13	0.294	1	Not significant
A*C*E*F	0.000044	0.000022	0.44	0.672	1	Not significant
A*D*E*F	0.000044	0.000022	0.44	0.672	1	Not significant
B*C*D*E	0	0	0	1	1	Not significant
B*C*D*F	-0.000112	-0.000056	-1.13	0.294	1	Not significant
B*C*E*F	-0.000081	-0.000041	-0.82	0.439	1	Not significant
B*D*E*F	-0.000069	-0.000034	-0.69	0.51	1	Not significant
C*D*E*F	-0.000031	-0.000016	-0.32	0.762	1	Not significant

[†] Note: 0 values in this table are a result of rounding off process by Minitab.

4.2.2 Normal Plot of the Effects

The normal probability plot is a tool to find out the direction, magnitude of the effects and the importance of them. According to the normal plot of the main effects and interaction effects which is shown in Figure 4.16, significant effects have been indicated with red square. The effects that lie along the straight red line are negligible and insignificant, while the important effects are far from the line. The significant effects derived from this analysis are the main effects of A, B, C, D and F and the AB, AC, AD, BC, BD, CD, ABC, ABD, ACD, BCD and ABCD interactions.

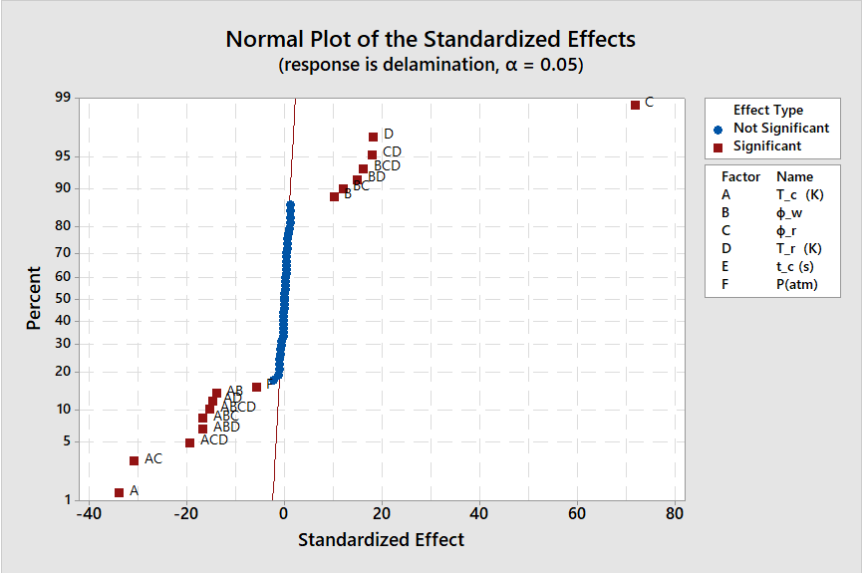

Figure 4.16: Normal probability plot of the effects.

4.2.3 Half Normal Plot

Half-normal plot of the effects is also obtained and shown in Figure 4.17. Similar significance of the effects can be interpreted in this plot compared to the normal probability plot. On the half-normal plot, the effect that are far from the line at

location of absolute standardized effect of 0 are statistically significant.

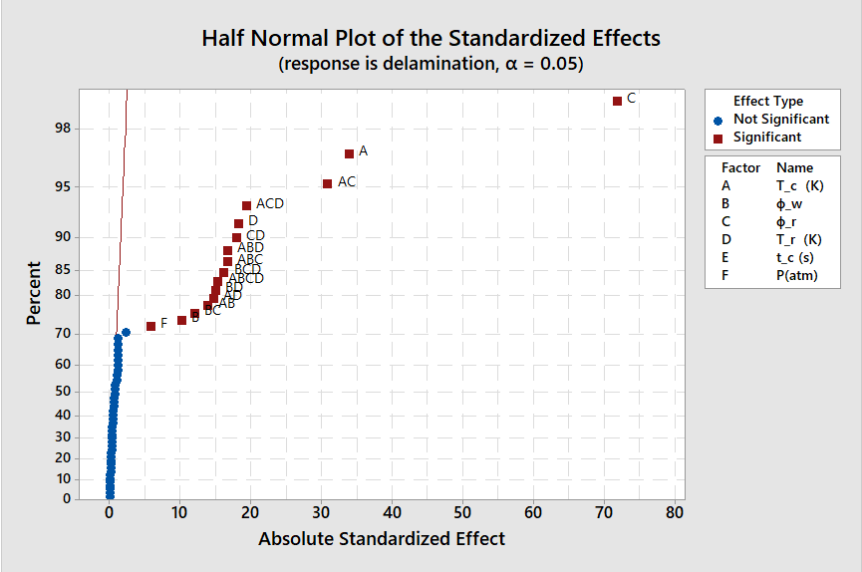

Figure 4.17: Half normal plot of the effects.

4.2.4 Pareto Chart

A Pareto chart is a kind of bar chart that organizes and arranges the absolute values and magnitude of the standardized effects from the largest and most significant effect to the smallest and least significant ones. The Pareto chart for this analysis is shown in Figure 4.18. If an effect passes the reference line standardized effect of 2.36 (shown with red dash line) then it can be considered as statistically important term affecting the results. The ones that are less than 2.36 are non-significant and negligible at the 0.05 *alpha level* with the current model terms. As an example, main effect C (humidity of room, ϕ_r) has the largest effect on the delamination following the main effect A (cooking temperature, T_c).

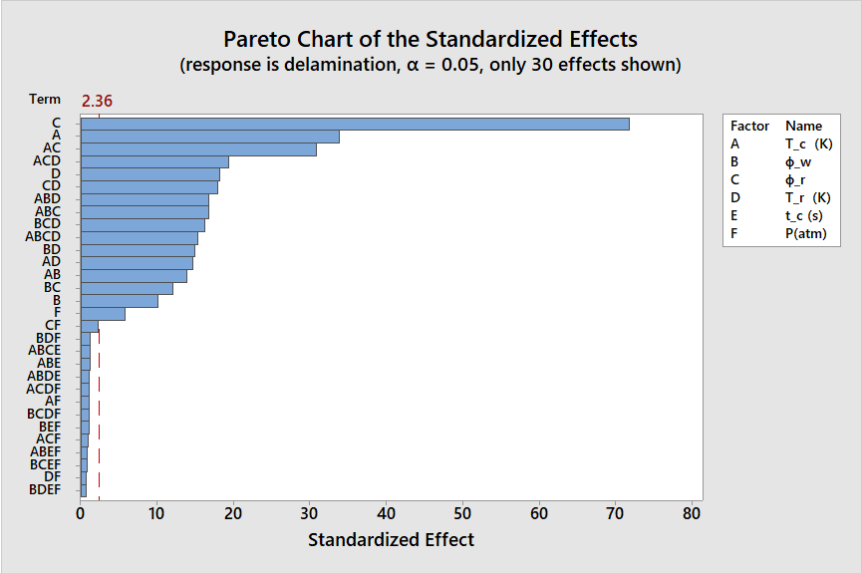

Figure 4.18: Pareto chart.

4.2.5 ANOVA Result

ANOVA results summarized in Table 4.9, was used to confirm the significant main and interaction effects statistically which is in agreement with the results from the normal and half normal probability plots and pareto chart.

P-value

When the *P-value* of an effect is small (less than the significance level, $\alpha = 0.05$), it means that effect is significant. A large value (more than $\alpha = 0.05$) indicates that effect is non-significant. Analysis of variance is presented in Table 4.9. As an example, the *P-value* of factor A (cooking temperature) is 0, which is less than 0.05. This shows that variable A is significant and different levels of cooking temperature are associated with delamination.

F-test

Another possible method to test the significance of the terms in ANOVA is the *F-test*.

$$F_{\text{Minitab}} = \frac{MS_{\text{Effect}}}{MS_{\text{Error}}} \tag{4.5}$$

Critical value of F is calculated as follows:

$$F_{\text{critical}} = F_{1-\alpha}\left(n_1, n_2\right) \tag{4.6}$$

where n_1 is the degree of freedom for numerator (DOF of that term) and n_2 is the degree of freedom for denominator (DOF of the error). If F_{computed} is bigger than F_{critical} , it is concluded that the factor is significant, otherwise it is insignificant. For instance, consider interaction effect AC. F_{computed} for AC is 950.51. n_1 for AC is 1 and n_2 is 7. By using F distribution table in (Montgomery, 2013, p. 690) $F_{0.05}(1, 7)$ is 5.59. Therefore, for interaction AC, F_{computed} is bigger than F_{critical} , thus AC is significant. In Table 4.9, the *F-value* of the model is 183.50 indicates that the model is significant. In this case, A, B, C, D, F, AB, AC, AD, BC, BD, CD, ABC, ABD, ACD, BCD, and ABCD are significant model terms.

Table 4.9: ANOVA table, first scenario.†

Source	*DF*	*Adj SS*	*Adj MS*	*F-Value*	*P-Value*	
Model	56	0.001616	0.000029	183.5	0	Significant
Linear	6	0.001065	0.000177	1128.66	0	Significant
A	1	0.00018	0.00018	1146.27	0	Significant
B	1	0.000016	0.000016	103.04	0	Significant
C	1	0.000811	0.000811	5156.87	0	Significant
D	1	0.000052	0.000052	332	0	Significant
E	1	0	0	0.14	0.716	Not significant
F	1	0.000005	0.000005	33.64	0.001	Significant
2-Way Interactions	15	0.000324	0.000022	137.26	0	
A*B	1	0.000031	0.000031	194.14	0	Significant
A*C	1	0.000149	0.000149	950.51	0	Significant
A*D	1	0.000034	0.000034	215.8	0	Significant
A*E	1	0	0	0.06	0.808	Not significant
A*F	1	0	0	1.29	0.294	Not significant
B*C	1	0.000023	0.000023	145.01	0	Significant
B*D	1	0.000035	0.000035	223.27	0	Significant
B*E	1	0	0	0.02	0.903	Not significant
B*F	1	0	0	0	1	Not significant
C*D	1	0.000051	0.000051	322.87	0	Significant
C*E	1	0	0	0.06	0.808	Not significant
C*F	1	0.000001	0.000001	5.15	0.058	Not significant
D*E	1	0	0	0.06	0.808	Not significant
D*F	1	0	0	0.57	0.474	Not significant
E*F	1	0	0	0.1	0.762	Not significant
3-Way Interactions	20	0.000189	0.000009	60.12	0	
A*B*C	1	0.000044	0.000044	279.15	0	Significant
A*B*D	1	0.000044	0.000044	279.15	0	Significant
A*B*E	1	0	0	1.59	0.248	Not significant
A*B*F	1	0	0	0.02	0.903	Not significant
A*C*D	1	0.000059	0.000059	374.64	0	Significant
A*C*E	1	0	0	0	1	Not significant
A*C*F	1	0	0	1.02	0.347	Not significant
A*D*E	1	0	0	0.4	0.548	Not significant
A*D*F	1	0	0	0.14	0.716	Not significant
A*E*F	1	0	0	0	0.951	Not significant
B*C*D	1	0.000041	0.000041	262.55	0	Significant
B*C*E	1	0	0	0.06	0.808	Not significant
B*C*F	1	0	0	0.06	0.808	Not significant
B*D*E	1	0	0	0.06	0.808	Not significant
B*D*F	1	0	0	1.59	0.248	Not significant
B*E*F	1	0	0	1.15	0.319	Not significant
C*D*E	1	0	0	0.25	0.629	Not significant
C*D*F	1	0	0	0.4	0.548	Not significant
C*E*F	1	0	0	0.1	0.762	Not significant
D*E*F	1	0	0	0.1	0.762	Not significant
4-Way Interactions	15	0.000038	0.000003	16.19	0.001	
A*B*C*D	1	0.000037	0.000037	234.72	0	Significant
A*B*C*E	1	0	0	1.59	0.248	Not significant
A*B*C*F	1	0	0	0	1	Not significant
A*B*D*E	1	0	0	1.29	0.294	Not significant
A*B*D*F	1	0	0	0.14	0.716	Not significant
A*B*E*F	1	0	0	0.67	0.439	Not significant
A*C*D*E	1	0	0	0.25	0.629	Not significant
A*C*D*F	1	0	0	1.29	0.294	Not significant
A*C*E*F	1	0	0	0.19	0.672	Not significant
A*D*E*F	1	0	0	0.19	0.672	Not significant
B*C*D*E	1	0	0	0	1	Not significant
B*C*D*F	1	0	0	1.29	0.294	Not significant
B*C*E*F	1	0	0	0.67	0.439	Not significant
B*D*E*F	1	0	0	0.48	0.51	Not significant
C*D*E*F	1	0	0	0.1	0.762	Not significant
Error	7	0.000001	0			
Total	63	0.001617				

† Note: 0 values in this table are a result of rounding off process by Minitab.

4.2.6 Factorial Plots

Main effects plot

Main effects plot is shown in Figure 4.19. It can be concluded from this plot that factor C (ϕ_r) is the most important factor in the pressing process as it shows the highest difference in mean of delamination at high and low levels. Increasing this factor will decrease the yield, hence increasing the delamination distance. Factor A (T_c) is the second most significant variable. This plot also shows that the main factor E (cooking time,t_c) is not significant in this experiment. Since the range of the cooking time is from 6 minutes to 9 minutes, this 3-minute difference does not affect the occurrence of the delamination defect. Therefore, in order to increase the production rate, it is preferred to set the pressing machine on 6 minutes. This plot indicates that initial moisture content of the wood, room humidity and room temperature have direct and positive effect. In other words, decreasing the amount of these factors will result in minimizing delamination. However, the main factors, cooking temperature and pressure, have negative effects which means decreasing the value of them will lead to increasing the distance of the delamination.

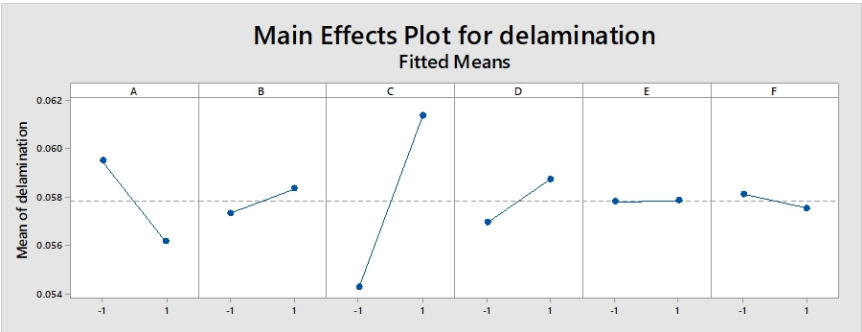

Figure 4.19: Main effects plot.

Interaction Plot

The interaction plot is presented in Figure 4.20. The interaction effect of cooking temperature (A) and room humidity (C) is the largest interaction effect. Parallel interaction lines indicate that there is no interaction and significant effect on delamination. When slopes of the lines are more different, their interaction is stronger.

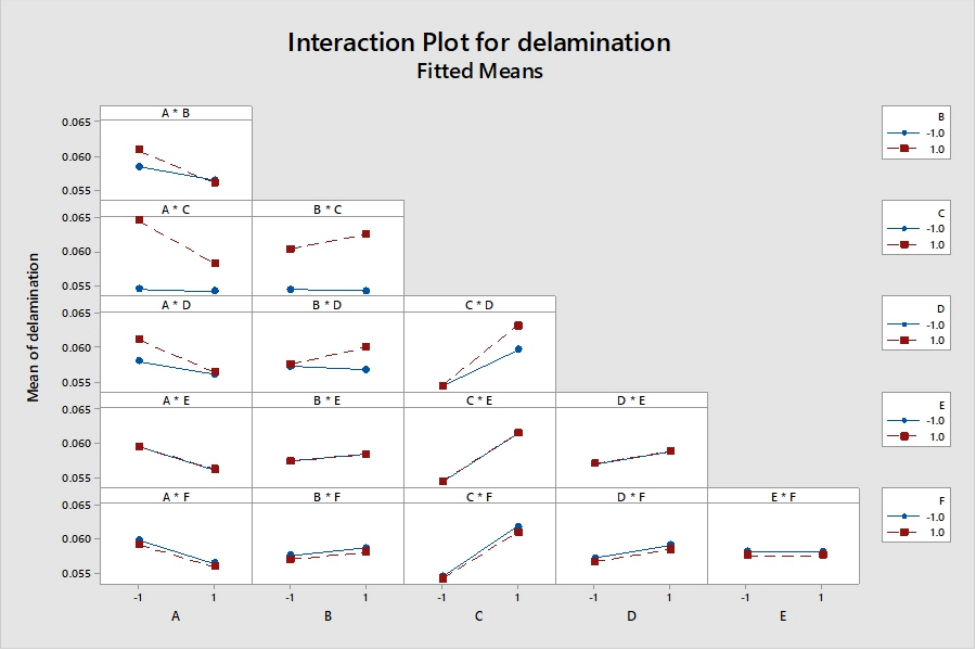

Figure 4.20: Interaction plot.

Contour, Surface and Cube Plots of Delamination

Contour, surface and cube plots of delamination are presented in Appendix A.

4.2.7 Normal Probability of the Residuals

The normal probability of the residuals for unrefined model is presented in Figure 4.21. The points on this plot are distributed closely to a straight line. The plot of residual

versus observation order is shown in Figure 4.22.

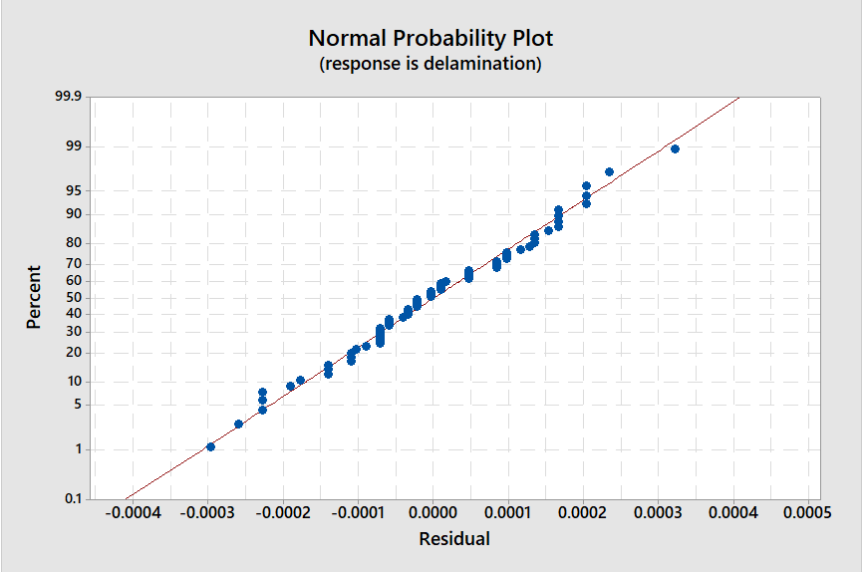

Figure 4.21: Normal probability plot of residuals for unrefined model.

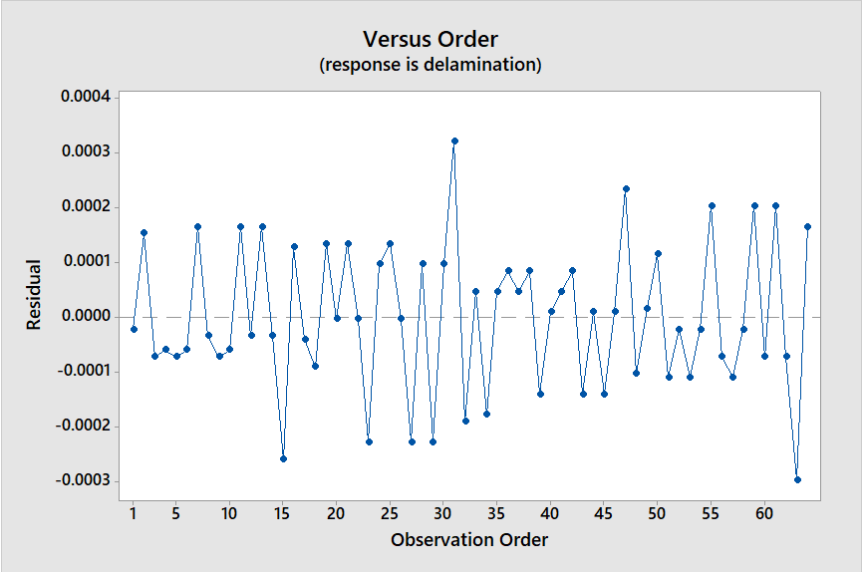

Figure 4.22: Residual versus observation order plot.

Model Summary Interpretation

S-value

In Table 4.10, S represents the average distance that the observed values deviate from the regression line. It determines how inaccurate the regression model is on average, using the units of the response variable. Smaller S values are better because it indicates that the observations are closer to the fitted line.

R-squared

R-squared is a statistical measure to determine the goodness of the fitted regression line. In general, higher the *R-squared* means that the model fits better to the data. *R-squared* is defined as the percentage of the response variable variation that is explained by a linear model:

$$R^2 = \frac{\text{Explained Variation}}{\text{Total Variation}} \tag{4.7}$$

R-squared is always between 0 and 100%. Calculated *R-squared* for the model in this work is 99.93% as shown in Table 4.10.

Table 4.10: Unrefined model summary.

S	R^2	R^2(adj)	R^2(pred)
0.0003965	99.93%	99.39%	94.31%

4.2.8 Design Projection

Design projection is another interpretation method to confirm the results in the first scenario when factor E and all interactions involving E were considered. Referring to our Minitab results presented above, variable E (cooking time) is unimportant and all interactions including E can be neglected, factor E can be removed from the experiment. Therefore, the new design converts to a 2^5 factorial in A, B, C, D, and F with two replicates. The drawn conclusion from this new design remains unchanged from the result when factor E is involved. All the significant effects have remained unchanged, however in this new scenario only one effect (interaction of room humidity and pressure) has been added to the to the set of significant effects. The reason is that in the un-replicated full factorial design, the effect of interaction of room humidity and pressure is very close to the reference line and with a slight change in the replicated design this effect has also become significant as all the errors are removed and the design has become more precise as a result. In other words, a single replicate of a 2^6 factorial design changed to a two replicated a 2^5 factorial design. Referring to the Pareto chart in Figure 4.23 of the new design, we draw the same conclusion as the un-replicated design. Both designs have the same significant effects. Note that factor E (cooking time) has been omitted.

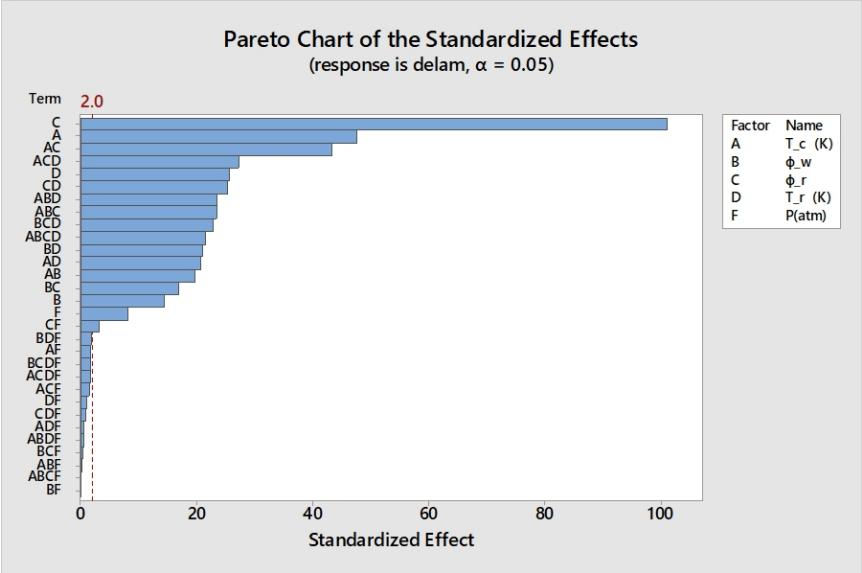

Figure 4.23: Pareto chart of design projection.

As the ANOVA table in the second scenario illustrates in Table 4.11, by neglecting the cooking time (factor E), the same results are obtained and the *P-value* of the *lack-of-fit* (0.382) shows it is lager than the *alpha* (0.05), which is the evidence of accepting the model correctly represents the relationship between the response and the predictors and the test does not detect any *lack-of-fit*.

Table 4.11: ANOVA table, second scenario (design projection).†

Source	*DF*	*Adj SS*	*Adj MS*	*F-Value*	*P-Value*	
Model	30	0.001614	0.000054	679.68	0	Significant
Linear	5	0.001065	0.000213	2689.89	0	Significant
A	1	0.00018	0.00018	2276.6	0	Significant
B	1	0.000016	0.000016	204.64	0	Significant
C	1	0.000811	0.000811	10242.01	0	Significant
D	1	0.000052	0.000052	659.38	0	Significant
F	1	0.000005	0.000005	66.82	0	Significant
2-Way Interactions	10	0.000324	0.000032	408.86	0	
AB	1	0.000031	0.000031	385.59	0	Significant
AC	1	0.000149	0.000149	1887.8	0	Significant
AD	1	0.000034	0.000034	428.6	0	Significant
AF	1	0	0	2.56	0.119	Not significant
BC	1	0.000023	0.000023	288.01	0	Significant
BD	1	0.000035	0.000035	443.44	0	Significant
BF	1	0	0	0	1	Not significant
CD	1	0.000051	0.000051	641.25	0	Significant
CF	1	0.000001	0.000001	10.23	0.003	Significant
DF	1	0	0	1.14	0.294	Not significant
3-Way Interactions	10	0.000188	0.000019	238.07	0	
ABC	1	0.000044	0.000044	554.41	0	Significant
ABD	1	0.000044	0.000044	554.41	0	Significant
ABF	1	0	0	0.03	0.86	Not significant
ACD	1	0.000059	0.000059	744.07	0	Significant
ACF	1	0	0	2.02	0.165	Not significant
ADF	1	0	0	0.28	0.598	Not significant
BCD	1	0.000041	0.000041	521.44	0	Significant
BCF	1	0	0	0.13	0.725	Not significant
BDF	1	0	0	3.16	0.085	Not significant
CDF	1	0	0	0.79	0.381	Not significant
4-Way Interactions	5	0.000037	0.000007	94.32	0	
$ABCD$	1	0.000037	0.000037	466.18	0	Significant
$ABCF$	1	0	0	0	1	Not significant
$ABDF$	1	0	0	0.28	0.598	Not significant
$ACDF$	1	0	0	2.56	0.119	Not significant
$BCDF$	1	0	0	2.56	0.119	Not significant
Error	33	0.000003	0			
Lack-of-Fit	1	0	0	0.78	0.382	Not significant
Pure Error	32	0.000003	0			
Total	63	0.001617				

† Note: 0 values in this table are a result of rounding off process by Minitab.

4.3 Regression Analysis

Regression equation is a statistical model that shows the relationship between independent (predictors) variables and a dependent (response) variable. It should be mentioned that based on the hierarchy principle, Minitab generates the regression model with high order terms of up to 4.

Refined Model

Model reduction or model refining is the process of elimination of terms from the model, whether they are predictor variables or their interactions. Model reduction simplifies the model and increases the precision of approximations. The refined model can be obtained from stepwise regression in Minitab software[1].

The regression equation is refined, and only significant factors are considered. This regression model shows the relationship between independent variables (predictors) and dependent variable (response). This mathematical model is non-linear with respect to independent variables due to the presence of interaction terms, however it is linear with respect to the coefficients. In Table 4.12, only significant terms are presented and the rest of the terms are considered as an error. In this table, $F\text{-}Value = 1018.46$ of the model indicates that the model is significant. It should be noted that the standard error of coefficient for the refined model is equal to 0.000039 which is less than the standard error of coefficient in the first scenario.

[1] https://support.minitab.com/en-us/minitab/18/help-and-how-to/modeling-statistics/regression/supporting-topics/regression-models/model-reduction/

Table 4.12: ANOVA table for delamination.

Source	*DF*	*Adj SS*	*Adj MS*	*F-Value*	*P-Value*
Model	16	0.001612	0.000101	1018.46	0
Linear	5	0.001065	0.000213	2152.39	0
A	1	0.00018	0.00018	1821.69	0
B	1	0.000016	0.000016	163.75	0
C	1	0.000811	0.000811	8195.44	0
D	1	0.000052	0.000052	527.62	0
F	1	0.000005	0.000005	53.47	0
2-Way Interactions	6	0.000323	0.000054	543.41	0
A*B	1	0.000031	0.000031	308.54	0
A*C	1	0.000149	0.000149	1510.58	0
A*D	1	0.000034	0.000034	342.95	0
B*C	1	0.000023	0.000023	230.46	0
B*D	1	0.000035	0.000035	354.83	0
C*D	1	0.000051	0.000051	513.11	0
3-Way Interactions	4	0.000188	0.000047	474.97	0
A*B*C	1	0.000044	0.000044	443.63	0
A*B*D	1	0.000044	0.000044	443.63	0
A*C*D	1	0.000059	0.000059	595.39	0
B*C*D	1	0.000041	0.000041	417.25	0
4-Way Interactions	1	0.000037	0.000037	373.02	0
A*B*C*D	1	0.000037	0.000037	373.02	0
Error	47	0.000005	0		
Total	63	0.001617			

As it can be seen in Table 4.13, the adjusted R^2 changes from 99.39% (in Table 4.10) to 99.61% as the insignificant terms are removed from the model.

Table 4.13: Refined model summary.

S	R^2	R^2(adj)	R^2(pred)
0.0003145	99.71%	99.61%	99.47%

The coded and uncoded (actual factors) refined expressions of delamination are shown in Equations 4.8 and 4.9, respectively.

$$\begin{aligned}\theta(\times 10000) = {} & 578.28 - 16.78A + 5.03B + 35.59C + 9.03D - 2.87F \\ & - 6.91AB - 15.28AC - 7.28AD + 5.97BC + 7.41BD + 8.91CD \\ & - 8.28ABC - 8.28ABD - 9.59ACD + 8.38BCD - 7.59ABCD\end{aligned} \tag{4.8}$$

$$\theta(\times 10000) = -6136.0 + 861.51T_c + 62334.0\phi_w + 12908.0\phi_r + 1084.5T_r - 0.14062P$$
$$- 167.57T_c\phi_w - 34.729T_c\phi_r - 2.9105T_cT_r - 2296.5\phi_w\phi_r - 210.54\phi_wT_r - 43.373\phi_rT_r$$
$$+ 6.182T_c\phi_w\phi_r + 0.56601T_c\phi_wT_r + 0.11671T_c\phi_rT_r + 7.735\phi_w\phi_rT_r - 0.020823T_c\phi_w\phi_rT_r \tag{4.9}$$

This uncoded equation is achieved by replacing each coded variable (P_{c}) with their equivalent uncoded expression in Equation 4.8 as follows:

$$P_{\mathrm{c}} = 2\left(\frac{U - U_{\min}}{U_{\max} - U_{\min}}\right) - 1 \tag{4.10}$$

where U is uncoded variable and $U_{\min}$ and $U_{\max}$ are lower and upper bounds of the uncoded variable, respectively. As an example, for the cooking temperature we have:

$$A = 2\left(\frac{T_c - 365.15}{6}\right) - 1$$

By replacing variable A in Equation 4.8 with this expression, the cooking temperature will be uncoded in this equation.

The conclusion from the regression model can be drawn that for minimizing delamination which is the goal of this research work, the cooking temperature (T_c) must be at its high level, the moisture content of the wood (ϕ_w) must be at its low level, the humidity of the room (ϕ_r) must be kept at its minimum value as possible, room temperature (T_r) must be remained at low level, and pressure (P) must be at its high value.

Normal probability plot of residuals from the refined model is presented in Figure. 4.24

which includes only significant terms. Also, since this plot is approximately linear, the error terms are normally distributed, which indicates the model is adequate. There is some mild tendency for the variance of the residuals at runs 31 and 63. Reexamination of the data did not reveal any obvious problem. Log data transformation was also performed on the results to deal with this minor problem; however it is not severe enough to have a dramatic impact on the analysis and conclusions.

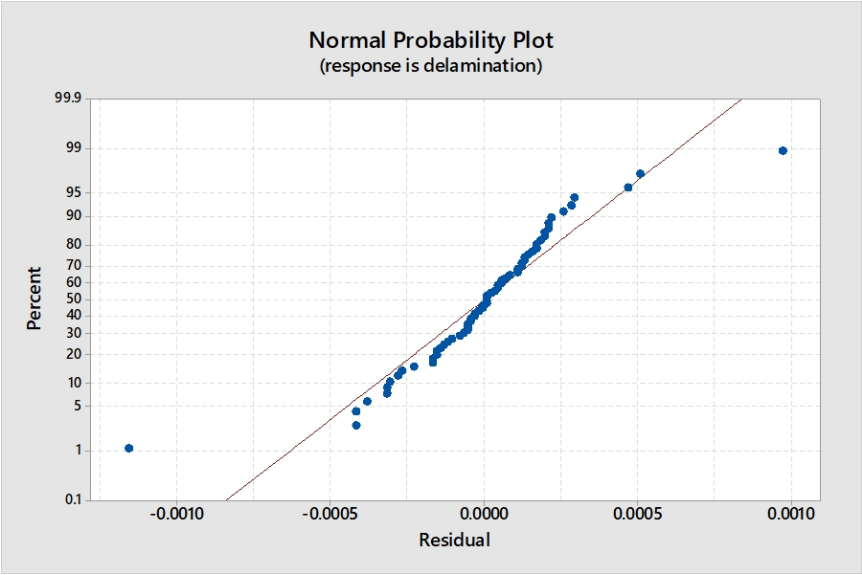

Figure 4.24: Normal probability plot of residuals for refined model.

Five numerical examples are tested in order to validate the regression model. Any value between -1 and +1 for each factor is acceptable to substitute in the coded regression model to obtain the value of delamination of the combination of the desired factors. On the other hand, the selected variables are used as input of the simulation and the value of delaminations are computed and compared with that of the regression model. The five sets of variables for the validation purpose are shown in Table 4.14.

Table 4.14: Variables for the model validation.

Test no.	Tc (K)	ϕ_w (%)	ϕ_r (%)	T_r (K)	t_c $(Sec.)$	P (atm)	θ_{model} (mm)
1	368.15	7	44	300.55	420	68.04	0.0569
2	366.65	8.5	58	298.65	520	81.65	0.0595
3	366.15	8	50	303.15	400	64.64	0.0606
4	370.15	8.7	48	301.15	500	78.25	0.0566
5	365.65	7.2	60	305.15	460	88.45	0.0633

As explained in Section 4.1, at first, moisture content of the veneer sandwich as well as the bonding strength are then computed. Results of this step are shown in Table 4.15.

Table 4.15: Moisture content and bonding strength for the validation scenarios.

Test no.	ϕ_e (%)	ϕ_c (%)	σ_e (MPa)	σ_c (MPa)	θ_{sim} (mm)
1	8	6.3	19.09	19.95	0.0570
2	10.6	8.79	17.77	18.69	0.0593
3	10.2	8.5	17.92	18.81	0.0589
4	8.1	6.2	19.01	19.96	0.0564
5	12.6	10.4	16.7	17.85	0.0636

Computed values of delamination from both the simulation (θ_{sim}) and refined model (θ_{model}) are shown in Table 4.16. It can be seen that the absolute modeling error is less than 3%.

Table 4.16: Computed delamination from simulation and refined model.

Test no.	θ_{sim} (mm)	θ_{model} (mm)	*Model error* (%)
1	0.0570	0.0569	-0.18
2	0.0593	0.0595	0.34
3	0.0589	0.0606	2.89
4	0.0564	0.0566	0.35
5	0.0636	0.0633	-0.47

Optimization with Matlab is conducted to confirm the results in the regression model

output. The obtained regression model is optimized in order to find the best variables' values which would result in minimum delamination. For this purpose, fmincon function of Matlab software is used. This method is gradient-based, which is suitable for problems with continuous objective and constraint functions as well as continuous first derivatives of these functions. For this optimization problem, only upper and lower bounds (lb and ub) are used on the variables. The coded regression model is used here; therefore the lb and ub are as follows:

$$\text{lb} = \begin{bmatrix} -1 & -1 & -1 & -1 & -1 & -1 \end{bmatrix}$$

$$\text{ub} = \begin{bmatrix} 1 & 1 & 1 & 1 & 1 & 1 \end{bmatrix}$$

The optimization is stopped after 44 iterations with optimality tolerance of 1e−6. The optimized parameter values are as follows:

A =0.9995

B = − 0.9982

C = − 0.9999

D = − 0.9991

F =0.9989

From these optimized values, it can be concluded that the minimum delamination occurs at high level of A, low level of B, C, D and high level of F. The delamination

value with these optimum variables is obtained as:

$$\theta_{\text{optim}} = 0.0534\ mm$$

Referring to Table 4.6 and Table 4.7, the minimum delamination happens at run number 34 ($\theta = 0.0535\ mm$), which is in agreement with the optimization results. However, since the design is replicated by removing the effect E, this result is observed again in run number 50 ($\theta = 0.0536\ mm$). Matlab code for optimization is presented in Appendix B. This setting recommendation is verified with response optimizer in Minitab as well.

4.4 Summary

In this chapter, the pressing process along with delamination defect using PVA adhesive were simulated. The possible root causes and the factors influencing the amount of delamination were analyzed and a regression model including the significant effects impacting delamination was proposed. It was concluded that the best value of variables were identified when A+, B-, C-, D-, F+ and factor E within its range (6 to 9 minutes) did not show any influence on the response. Thus, for accelerating the production rate and reducing the cost, 6 minutes of pressing process is preferred. For testing the regression model, 5 numerical examples were provided. Similar simulation with UF adhesive was also performed; however, since UF is insensitive to moisture content, changes in delamination was negligible.

Chapter 5

Conclusion and Future Work

This chapter draws the main conclusions obtained in this work. Prospective points for the future work of this research are recommended as well.

5.1 Conclusion

In this thesis, simulation of hot-press plywood and design of experiment of the controllable parameters causing the delamination defect in the pressing stage are investigated. The goal of solving the mathematical model is to minimize the amount of delamination according to the optimum value of the variables. In order to gain the minimum delamination, the amount of the delamination defect is treated as a response to determine and optimize the occurrence of the distance between the veneer layers. A classical DOE technique is selected to find the effective factors on delamination in specific ranges. ANOVA reveals that the humidity of the room is the most significant

factor that affects the amount of delamination followed by cooking temperature, in comparison with the other factors such as room temperature, moisture content of the wood and the pressure. Cooking time is insignificant, which means that it does not affect delamination within the defined range.

5.2 Future Work

There are various recommendations in order to extend this research work. For future work, the following are recommended:

- The mathematical model presented in this thesis can be developed for other types of wood with this methodology as long as the mechanical properties of them are available.
- This simulation and modeling can be conducted for analyzing other types of defects.
- Dehumidifier can be used in the pressing shop to examine the reduction of room humidity affecting delamination.
- Chemical pretreatments can be applied to wood surfaces in order to reduce the possibility of debonding. This allows us to improve bonding and wettability. Besides, cold pressing can be considered as a pre-press step which helps to even out the moisture level.
- Temperature and pressure sensors can be installed in the plywood package to

investigate whether the temperature and pressure are distributed uniformly and evenly.

- Non-destructive tests and measurements can be periodically conducted after each step of production to prevent any potential defect to pass to the subsequent steps.

Bibliography

[1] J. Aderhold and B. Plinke. *Innovative Methods for Quality Control in the Wood-Based Panel Industry*, chapter 6. London: Brunel Univ. Press, 2010.

[2] T. Bardak, E. Sozen, K. Kayahan, and S. Bardak. The Impact of Nanoparticles and Moisture Content on Bonding Strength of Urea Formaldehyde Resin Adhesive. *Drvna industrija*, 69(3):247–252, 2018.

[3] P. Bekhta, S. Hiziroglu, and O. Shepelyuk. Properties of plywood manufactured from compressed veneer as building material. *Materials & Design*, 30(4):947–953, 2009.

[4] L. Blomqvist, J. Johansson, and D. Sandberg. Shape stability of laminated veneer products An experimental study of the influence on distortion of some material and process parameters. *Wood Material Science and Engineering*, 8(3): 198–211, 2013.

[5] V. V. Bolotin. Delaminations in composite structures: its origin, buckling, growth and stability. *Composites Part B: Engineering*, 27(2):129–145, 1996.

[6] J. Bomba, P. edivka, M. Bhm, and M. Devera. Influence of moisture content on the bond strength and water resistance of bonded wood joints. *BioResources*, 9 (3):5208–5218, 2014.

[7] G. E. P. Box, J. S. Hunter, and W. G. Hunter. Chapter 5. Factorial Design at Two Levels. In *Statistics for experimenters: design, innovation, and discovery*, Wiley series in probability and statistics. Wiley-Interscience, Hoboken, N.J, 2nd edition, 2005.

[8] B. K. Brashaw, V. Bucur, and F. Divos. Nondestructive testing and evaluation of wood: A worldwide research update. *Forest products journal. Vol. 59, no. 3 (Mar. 2009): pages 7-14.*, 59(3):7–14, 2009.

[9] D. Brouse. Some causes of warping in plywood and veneered products. Technical Report U. S. Forest Service Research Note FPL-0136, Forest Products Laboratory, Forest Service U.S. Department of Agriculture, 1966.

[10] V. Bucur and D. Lloyd. *Delamination in Wood, Wood Products and Wood-Based Composites*, chapter 1, 2, 6. Springer, Dordrecht, 2011.

[11] A. Buikis, J. Cepitis, and S. Kostjukova. The mathematical model of the plywood production. In *WSEAS International Conference Proceedings Mathematics and Computers in Science and Engineering*. WSEAS, 2008.

[12] M. D. Burnard, L. Muszyski, S. Leavengood, and L. Ganio. An optical method for

rapid examination of check development in decorative plywood panels. *European Journal of Wood and Wood Products*, 76(5):1367–1377, 2018.

[13] E. O. Cakiroglu, A. Demir, and I. Aydin. Comparison of birch and beech wood in terms of economic and technological properties for plywood manufacturing. *Drvna industrija*, 70(2):169–174, 2019.

[14] P. Cavalin, L. S. Oliveira, A. L. Koerich, and A. S. Britto. Wood defect detection using grayscale images and an optimized feature set. In *IECON 2006 - 32nd Annual Conference on IEEE Industrial Electronics*, pages 3408–3412, Paris, France, 2006. IEEE.

[15] J. J. del Coz Díaz, P. G. Nieto, A. L. Martínez-Luengas, F. S. Domínguez, and J. D. Hernández. Non-linear numerical analysis of plywood board timber connections by DOE-FEM and full-scale experimental validation. *Engineering Structures*, 49:76–90, 2013.

[16] A. Delgado, J. de Brito, and J. D. Silvestre. Inspection and Diagnosis System for Wood Flooring. *Journal of Performance of Constructed Facilities*, 27(5): 564–574, 2013.

[17] A. EL Moustaphaoui, A. Chouaf, M. Chergui, and K. Kimakh. Modeling of macroscopic delamination of plywood using design of experiments method. *Journal of the Indian Academy of Wood Science*, 16(2):144–154, 2019.

[18] J. Hrázskỳ, P. Král, et al. Analysis of causes of warping the plywood sheets.

Acta Universitatis Agriculturae et Silviculturae Mendelianae Brunensis, 59(3): 59–72, 2011.

[19] I. V. Ivanov, T. Sadowski, M. Filipiak, and M. Kne. Experimental and numerical investigation of plywood progressive failure in CT tests. *Budownictwo i Architektura*, 2:79–94, 2008.

[20] A. Kovryga, P. Stapel, and J. W. G. van de Kuilen. Mechanical properties and their interrelationships for medium-density European hardwoods, focusing on ash and beech. *Wood Material Science & Engineering*, pages 1–14, 2019.

[21] M. Kymäläinen, A. Yamamoto, K. Sokka, and L. Rautkari. The effect of compression and incision on wood veneer and plywood physical and mechanical properties. *Wood Material Science & Engineering*, pages 1–7, 2018.

[22] A. Lavalette, A. Cointe, R. Pommier, M. Danis, C. Delise, and G. Legrand. Experimental design to determine the manufacturing parameters of a green-glued plywood panel. *European Journal of Wood and Wood Products*, 74(4):543–551, 2016.

[23] F. Louvet and L. Delplanque. *Les plans d'expérience: une approchepragmatique et illustrée (Experimental designs: an illustrated andpragmatic approach) (In French)*. Association Expérimentique, Orléans, 2005.

[24] A. Magnevik. Numerical simulation of moulding and distortion in hot-pressed

veneer products. Master's thesis, Chalmers University of Technology, Gteborg, Sweden, 2006.

[25] P. Meinlschmidt. Thermographic detection of defects in wood and wood-based materials. In *14th International Symposium of Nondestructive Testing of Wood*, Honnover, Germany, 2005.

[26] F. Mirianon, S. Fortino, and T. Toratti. *A method to model wood by using ABAQUS finite element software. Part 2. Application to dowel type connections.* VTT Technical Research Centre of Finland, 2008.

[27] D. C. Montgomery. *Introduction to Statistical Quality Control.* John Wiley & Sons, Inc., 7th edition, 2012.

[28] D. C. Montgomery. *Design and analysis of experiments.* John Wiley & Sons, Inc, Hoboken, NJ, 8th edition, 2013.

[29] S. Ormarsson and D. Sandberg. Numerical simulation of hot-pressed veneer products: moulding, spring-back and distortion. *Wood Material Science and Engineering*, 2(3-4):130–137, 2007.

[30] R. J. Ross, B. K. Brashaw, and R. F. Pellerin. Nondestructive evaluation of wood. *Forest products journal*, 48(1):14, 1998.

[31] C. Salinas, R. Ananas, and D. A. Vasco. Modelling of radio-frequency heating of piles of pinus radiata wood. *BioResources*, 13(1):945–953, 2017.

[32] A. Schramm. *A complete guide to hardwood plywood and face veneer.* Purdue University Press, West Lafayette, Ind, 2003.

[33] F. Stoeckel, J. Konnerth, and W. Gindl-Altmutter. Mechanical properties of adhesives for bonding woodA review. *International Journal of Adhesion and Adhesives*, 45:32–41, 2013.

[34] A. M. Taylor, S. H. Baek, M. K. Jeong, and G. Nix. Wood shrinkage prediction using NIR spectroscopy. *Wood and Fiber Science*, 40(2):301–307, 2008.

[35] A. TenWolde, J. D. McNatt, and L. Krahn. Thermal properties of wood and wood panel products for use in buildings. Technical report, Oak Ridge National Lab., TN (USA); Forest Service, Madison, WI (USA), 1988.

[36] H. Thoemen, editor. *Wood-based panels: an introduction for specialists.* Brunel Univ. Press, London, 2010.

[37] C. B. Vick. Adhesive bonding of wood materials. *Wood handbook: wood as an engineering material. Madison, WI: USDA Forest Service, Forest Products Laboratory, 1999. General technical report FPL; GTR-113: Pages 9.1-9.24*, 113, 1999.

Appendices

Appendix A

Contour, Surface and Cube Plots of Delamination

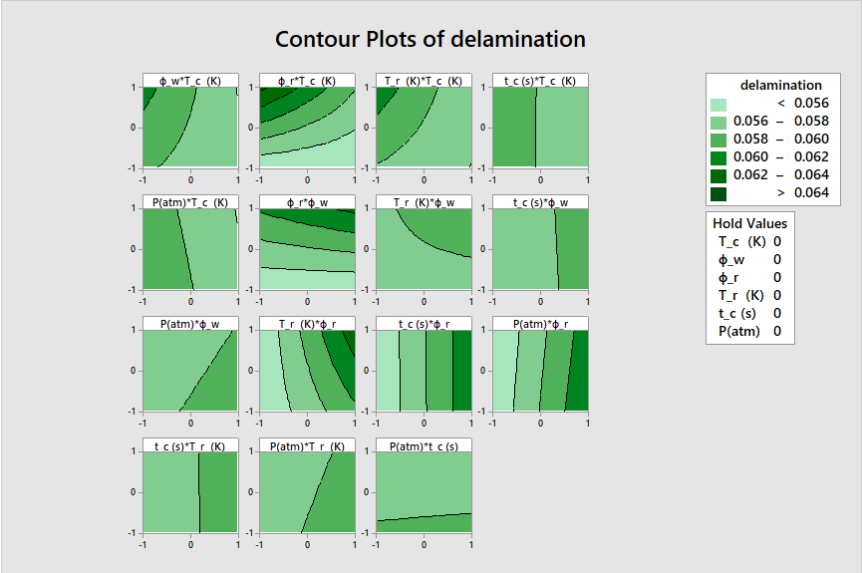

Figure A.1: Contour plots of delamination.

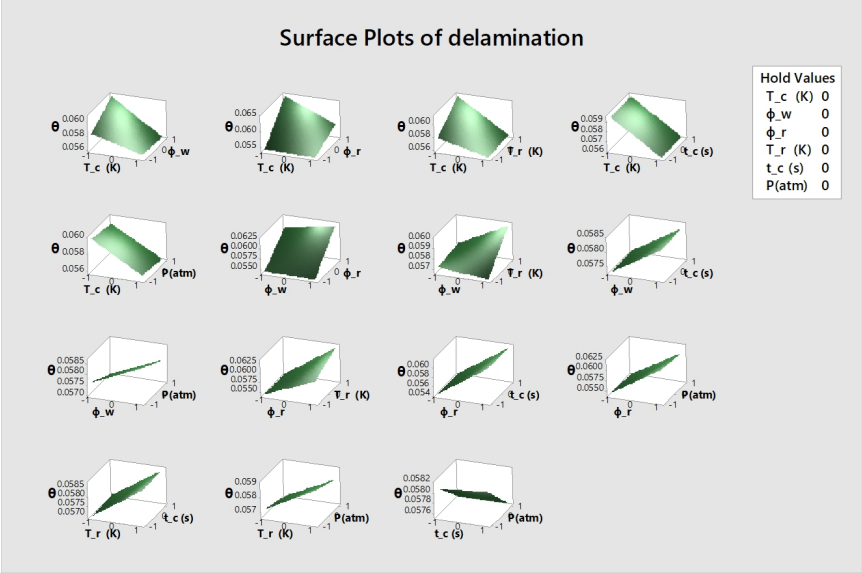

Figure A.2: Surface plots of delamination.

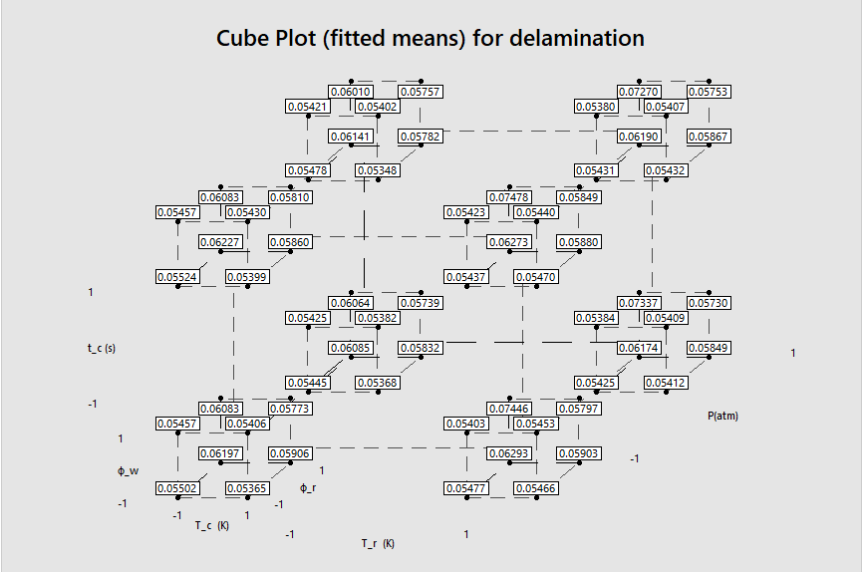

Figure A.3: Cube plots of delamination.

Appendix B

MATLAB Code for Parameter Optimization

Begin (optim.m)

```
% Clear the workspace
clear all;
clc;
% Set optimizer options for fmincon
options = optimoptions('fmincon');
options = optimoptions(options,'Display', 'iter');
% Run fmincon optimization and print the results
optim_params = fmincon(@delam_fun, [0 0 0 0 0], [], [], [], [], ...
[-1 -1 -1 -1 -1], [1 1 1 1 1],[],options)
% Print delamination value with the optimized parameters
del = delam_fun(optim_params)

function del = delam_fun(params)
A=params(1);
B=params(2);
C=params(3);
D=params(4);
F=params(5);
del = 0.057828 - 0.001678*A + 0.000503*B + 0.003559*C + 0.000903*D -
    0.000287*F - 0.000691*A*B - 0.001528*A*C - 0.000728*A*D +
        0.000597*B*C + 0.000741*B*D + 0.000891*C*D - 0.000828*A*B*C -
        0.000828*A*B*D - 0.000959*A*C*D + 0.000803*B*C*D -
        0.000759*A*B*C*D;
end
```

End (optim.m)